

# Heavy Quarkonia in Quark-Gluon Plasma

Cheuk-Yin Wong

Physics Division, Oak Ridge National Laboratory, Oak Ridge, TN 37831 and

Department of Physics, University of Tennessee, Knoxville, TN 37996

(Dated: December 24, 2018)

Using the color-singlet quark-antiquark potential obtained by Kaczmarek et al. from quenched lattice QCD theory, we study the binding energies and wave functions of heavy quarkonia in quark-gluon plasma above the transition temperature  $T_c$ . We find that  $J/\psi$  dissociates spontaneously at  $2T_c$ ,  $\psi'$  at  $1.2T_c$ , at  $4.5T_c$ , and  $\chi_c$  and  $\psi_c$  at  $2T_c$ . A comparison of the dissociation temperatures in this potential model analysis and the spectral function analyses of Asakawa et al. and Petreczky et al. indicates qualitative agreement that  $J/\psi$  and  $\psi'$  are stable at a temperature slightly above  $T_c$  and dissociate spontaneously at higher temperatures. It is, however, not necessary to reach the temperature for spontaneous dissociation with zero binding energy for a quarkonium to dissociate. A quarkonium can dissociate by thermalization and by collision with gluons in quark-gluon plasma. We evaluate the cross section for  $J/\psi$  dissociation in collision with gluons,  $(g + J/\psi \rightarrow c + \bar{c})$ , and calculate the  $J/\psi$  collisional dissociation rate and collisional dissociation width. The  $J/\psi$  binding energy is equal to its collisional dissociation width at  $1.2T_c$ , indicating a strong instability for  $J/\psi$  collisional dissociation if the temperature greatly exceeds  $1.2T_c$ . To study the production of  $J/\psi$  by the recombination of charm quarks and antiquarks, we calculate the cross section for the reaction  $c + \bar{c} \rightarrow g + J/\psi$  and determine the rate of  $J/\psi$  production arising from the collision of charm quarks and antiquarks in quark-gluon plasma.

PACS numbers: 25.75.-q 25.75.Dw

## I. INTRODUCTION

The stability of heavy quarkonia in the quark-gluon plasma is an interesting subject of current research in high-energy heavy-ion collisions as Matsui and Satz suggested that the suppression of  $J/\psi$  production can be used as a signature of the quark-gluon plasma [1]. DeTar [2, 3], Hansson, Lee, and Zahed [4] argued however that because the range of strong interaction is not likely to change drastically across the phase transition, low-lying mesons including  $J/\psi$  may remain relatively narrow states and the suppression of  $J/\psi$  is not a signature of the deconfinement phase transition [3]. Whether or not  $J/\psi$  production will be suppressed depends on the screening between the heavy quark and the heavy antiquark when the quarkonium is placed in the quark-gluon plasma. The degree of screening is highly nonperturbative at temperatures near the phase transition temperature [5]. The related question of the quarkonium stability must be examined in nonperturbative QCD using, for example, the lattice-gauge theory.

Recent investigations of masses and widths of heavy quarkonia in quenched lattice QCD calculations were carried out by Asakawa et al. [6, 7] and Petreczky et al. [8, 9, 10] using spectral function analysis and the maximum entropy method. They found that the width of  $J/\psi$  remains relatively narrow up to 1.6 times the critical phase transition temperature  $T_c$ . Reconsidering the properties of the quark-gluon plasma also led Zahed and Shuryak to suggest that quark-gluon plasma at temperatures up to a few  $T_c$  supports weakly bound meson states [11, 12, 13, 14]. They have also estimated the binding energy of  $J/\psi$  and found it to be stable up to  $2.7T_c$  [12]. The possibility of weakly bound meson states in the quark-gluon plasma was suggested earlier by DeTar [2, 3], Hatsuda, and Kunihiro [15]. Phenomenological discussions on medium modifications of charmonium in high-energy heavy-ion collision have been presented recently by Grandchamp, Rapp, and Brown [16].

As the knowledge of the stability of  $J/\psi$  has important implications on the fate of  $J/\psi$  in quark-gluon plasma, it is important to obtain an independent assessment on the binding of heavy quarkonia, in addition to those from previous analyses. The spectral analyses of heavy quarkonia using gauge-invariant current-current correlators have been carried out in the quenched approximation. The change in the stability of these systems arises from the screening (or perhaps even antiscreening) of the  $Q\bar{Q}$  interaction due to deconfined gluons. Within the quenched approximation, independent lattice-gauge theory calculations have also been carried out using the correlation of Polyakov lines from which the free energy and the two-body potential between  $Q$  and  $\bar{Q}$  can be calculated [17]. The two-body potential obtained from the lattice-gauge theory in such an approach can be used to study the dissociation of heavy quarkonia. It is of interest to ask whether, within the same quenched approximation, the spectral analysis and the potential model analysis lead to consistent results concerning the stability of quarkonia in the quark-gluon plasma.

Besides checking the consistency of independent quenched lattice-gauge calculations, we would like to use the potential model to examine many physical quantities of interest. If quarkonia are indeed stable in the plasma, it is useful to find out how strongly bound they are. The binding energies of a heavy quarkonium, in comparison with

the magnitude of the temperature, provide an assessment on the degree of its stability, as a heavy quarkonium can dissociate by thermalization in the quark-gluon plasma [18, 19, 20]. Furthermore,  $J/\psi$  can dissociate by collision with constituents of the plasma. In such a collisional dissociation, the rate of dissociation depends on the cross section for the reaction  $g + J/\psi \rightarrow c + c$ . We would like to evaluate this cross section as a function of temperature  $T$ , which can be obtained by using the bound state wave functions in the potential model. The knowledge of the dissociation cross section allows a determination of the collisional dissociation width. A comparison of the magnitude of the binding energy with the collisional dissociation width provides an additional assessment of the stability of heavy quarkonia in the quark-gluon plasma.

In energetic heavy-ion collisions, many pairs of charm quarks and antiquarks may be produced in a single central collision [21, 22]. These charm quarks and antiquarks can recombine to form  $J/\psi$  in the quark-gluon plasma. We also wish to find out here the rate of producing  $J/\psi$  through such a reaction. The production rate depends on the cross section for the reaction  $c + c \rightarrow J/\psi + g$ . The latter quantity can be obtained from the cross section for the inverse reaction  $g + J/\psi \rightarrow c + c$ , which we already intend to calculate.

Previously, the effects of temperature on the stability of heavy quarkonium was studied by Digalet et al. [23, 24] and Wong [19, 20] using the free energy and assuming that the effects of entropy are small. It was, however, pointed out by Zantov, Kaczmarek, Karsch and Petreczky [5, 25] that the effects of entropy depend on the separation of  $c$  and  $c$ , and the internal energy function, instead of the free energy, should be used as the interaction potential for the calculation of heavy quarkonium bound states. We shall follow Zantov et al. [25] and adopt such an approach for this investigation.

When a heavy quarkonium is placed in a quark-gluon plasma, conventional description assumes that the medium effect is dominated by the effect of Debye screening [1, 5], which leads to a decrease in the attractive interaction between the heavy quark and antiquark. Not much attention, however, is focused on the effects of antiscreening due to the deconfined gluons. It is of interest to investigate the antiscreening effects arising from deconfined gluons.

We would like to show that because the Gauss law of QCD contains a non-linear term involving the gluon field, the gluon field induces color charges at the field points. These induced color charges act to antiscreen the interaction between the heavy quark and the antiquark. We shall show that the strength of the antiscreening effect increases with an increase in the gluon correlation length and is proportional quadratically to the magnitude of the gluon fields. The antiscreening effects due to deconfined gluons brings a new degree of freedom to mediate the interaction between the quark and the antiquark. We shall examine the signature of antiscreening and see whether antiscreening may be related to the strong coupling between the heavy-quark and antiquark at  $T$  slightly greater than  $T_c$  found in lattice gauge results.

This paper is organized as follows. In Section II, we review the heavy quarkonium production mechanism and the thermalization of the quark-gluon medium in high-energy heavy-ion collisions. We examine the evidence for rapid thermalization as revealed by the elliptic flow and hydrodynamics. In Section III, we review the lattice gauge calculations for the interaction between a heavy quark and antiquark and the gauge dependence of the interaction in bound state problems. In Section IV, we show how the color-singlet  $Q\bar{Q}$  potential obtained by Kaczmarek et al. [17] in quenched QCD can be parameterized as a screened color-Coulomb potential. We discuss the meaning of the parameters extracted from the lattice gauge results and investigate the effects of antiscreening due to deconfined gluons in the quark-gluon plasma in Section V. Using the heavy quark-antiquark potential, we calculate the eigenenergies and eigenfunctions for charmonia in quark-gluon plasma as a function of temperature in Section V I. The location of the temperature at which a quarkonium begins to be unbound is then determined as the spontaneous dissociation temperature of the quarkonium. The temperatures for spontaneous dissociation of  $J/\psi$  and  $\psi'$  are compared with the dissociation temperatures determined from spectral analyses. In Section V II, we calculate the eigenenergies and eigenfunctions for  $(b\bar{b})$  bound states in quark-gluon plasma as a function of temperature. In Section V III, we use the  $J/\psi$  bound state wave function to calculate the cross section for  $g + J/\psi \rightarrow c + c$  after the  $J/\psi$  absorbs an E1 gluon, using the formulation of gluon dissociation cross section presented previously [20]. The collisional dissociation width of  $J/\psi$  in the quark-gluon plasma is then determined as a function of temperature in Section IX. We compare the  $J/\psi$  collisional dissociation width with the binding energy to provide an assessment of the stability of heavy quarkonia in quark-gluon plasma. In Section X we evaluate the cross section for the inverse process of  $c + c \rightarrow J/\psi + g$  using the cross section of  $g + J/\psi \rightarrow c + c$  obtained in Section V III. The rate of  $J/\psi$  production by recombining  $c$  and  $c$  in a quark-gluon plasma is estimated. We conclude our discussions in Section X I.

## II. HEAVY QUARKONIA PRODUCTION AND THE THERMALIZATION OF THE MEDIUM

We are interested in using a heavy quarkonium to probe the properties of the matter produced in central high-energy heavy-ion collisions. In the collision frame, the colliding nuclei have the shape of Lorentz-contracted disks. The collisions are known to be highly inelastic in which a large fraction of the incident collision energy is released after

the collision. What is the rate of the relaxation of the initial configuration to thermal equilibrium?

From the experimental viewpoint, recent RHIC experiments by the STAR [26], PHENIX [27], and PHOBOS [28] Collaborations reveal the presence of an elliptic collective flow in non-central Au-Au collisions at RHIC energies. The occurrence of such a flow indicates that the initial azimuthally symmetric momentum distribution of particles is deformed into an azimuthally asymmetric momentum distribution. The magnitude of the azimuthally asymmetry is sensitive to the time at which the free streaming of particles terminates and the dynamics of a thermally equilibrated system begins [29, 30, 31]. Too late a thermalization time will lead to a spatially more extended system with a lower pressure gradient and a smaller azimuthal asymmetry. It is also sensitive to the numbers of degrees of freedom in the equation of state. The magnitude of the azimuthal asymmetry can be well explained in terms of a hydrodynamical model of the quark-gluon plasma by assuming thermalization at an initial time about 0.6 fm/c [29]. We infer from the experimental data of the elliptic flow and its theoretical description in terms of hydrodynamics that the thermalization in the central region of a RHIC nucleus-nucleus collision is very rapid, as short as 0.6 fm/c after the collision.

From theoretical viewpoints, it was first pointed out by Landau [32] that the initial configuration after a high-energy nuclear collision consists of matter at an extremely high energy density in a very thin disk. The great magnitude of the energy density means that the number density of quanta of matter is very large. Such a large number density in the thin disk of matter leads to a very mean-free-path compared to its dimensions, leading to a rapid relaxation to thermal equilibrium. According to Landau, "in the course of time, the system expands, the property of the mean-free path must be valid also for a significant part of the process of expansion and this part of the expansion process must have hydrodynamical character" [32]. Landau hydrodynamics provides a reasonable description of the widths of the rapidity distribution for high-energy hadron-hadron and nucleus-nucleus collisions from  $\sqrt{s} = 3$  GeV to RHIC collisions at 200 GeV [33, 34]. Hydrodynamical description with a rapid thermal relaxation also provides a good description of the elliptic flow of matter after a Au-Au collision at RHIC, as indicated above.

It is also useful to point out that a quanta in the non-equilibrium QCD matter interacts not only with other quanta (gluons and quarks) in two-body processes in terms of two-body collisions, but the quanta also interact with the fields generated by all other quanta. Because of the non-Abelian nature of the QCD interaction, the fields generated by other quanta are also sources of color fields and the quanta must in addition interact with the color fields generated by the fields of all other particles, in a highly non-linear manner (see Section V for another manifestation of the non-linear nature of the gauge field). Thus, a quanta interacts with other quanta not only by direct short-range two-body collisions, but also by highly non-local action-at-a-distance long-range interactions, through the fields generated by the fields of other quanta. There is thus an additional non-linear and long-range mechanism of thermalization in non-Abelian interactions which provides an extra push for rapid relaxation to thermal equilibrium.

The rate of thermalization of a quark-gluon system after an ultra-relativistic heavy-ion collision is the subject of current theoretical research and has been discussed by Wong [35], Molnar, and Gyulassy [36]. The mean-free-path has also been discussed by Shuryak [37], Gyulassy and McLerran [38], (see also Ref. [39]). The focus of the research is on trying to understand the phenomenologically fast rate of thermalization as indicated by the experimental elliptic flow evidence. For example, in the work of Molnar and Gyulassy [36], it was necessary to shorten the parton mean-free-path by an order of magnitude in order to reproduce the magnitude of the elliptic flow. Similarly, in the work of Lin, Ko, and Pal [40] in parton cascade, it was necessary to increase the parton-parton cross section by a large factor to describe the dynamics in a nucleus-nucleus collisions at RHIC.

To use heavy quarkonia as a probe of the quark-gluon plasma, we need a knowledge of the heavy-quarkonium production mechanism. In a nucleus-nucleus collision at high energies, the partons of one nucleon and the partons of another nucleon can collide to produce occasionally a pair of heavy quark and antiquark. The time scale for the production is of the order of  $\sim=2m_Q$  where  $m_Q$  is the mass of the heavy quark. It is of order 0.06 fm/c for a c-c pair and of order 0.02 fm/c for a b-b pair. As the initial partons carry varying fractions of the initial momenta of the colliding nucleons, the heavy quark pair will come out at different energies. Depending on the Feynman diagram of the production process, the produced Q-Q pair after the hard scattering process may be in a purely color-singlet quarkonia state or a coherent admixture of color singlet- and color-octet states [41, 42]. The projection of different states from a coherent admixture gives the probability amplitude for the occurrence of the final states. A color-octet state will need to emit a soft gluon of energy  $E_{\text{gluon}}$  to become subsequently a color-singlet state in an emission time of order  $\sim=E_{\text{gluon}}$ . For the emission of soft gluon of a few hundred MeV, the time for the emission is of order 0.5-1.0 fm/c.

From the above considerations on the rapid thermalization of the quark-gluon plasma and the time for the production of heavy quarkonia, one envisages that by the time when the colliding matter is thermalized at about 0.6 fm/c, a large fraction of the quarkonia have already been formed, although in various energy states. The quark-gluon plasma is expected to have a life time of a few fm/c which is longer than the heavy quarkonium orbital period of order  $\sim=0.5$  GeV. It is therefore meaningful to study the fate of a produced heavy quarkonia in a thermalized quark-gluon plasma at a finite temperature. The behavior of the heavy quarkonium system before thermal equilibrium and the interaction of a coherent Q-Q color admixture in the quark-gluon plasma are other topics which are beyond the scope of the

investigation of the present manuscript.

### III. LATTICE-GAUGE CALCULATIONS

In a quark-gluon plasma, a quarkonium is actually a heavy quark and a heavy-antiquark each surrounded by a cloud of gluons and quarks. In the quenched approximation in which there are no dynamical quarks, the cloud surrounding the heavy quark and antiquark is approximated to consist of gluons only. As gluons are involved, the quark-antiquark system will be in different color states at different instances. We shall be interested in those systems in which the heavy-quark and antiquark exist in the color-singlet state. Only in the color-singlet state will be the effective interaction between a quark (plus its cloud) and an antiquark (plus its cloud) be attractive. Such a color-singlet system can further absorb a gluon and become a color-octet system and we shall also study the cross section for such a process.

The interaction between a heavy quark and a heavy antiquark in the color-singlet state,  $V_1(r;T)$ , was studied by Kaczmarek, Karsch, Petreczky, and Zantow [17]. They calculated  $hTrL(x)L^Y(0)$  in the quenched approximation and they obtained the color-singlet free energy  $F_1(x;T)$  from

$$hTrL(x)L^Y(0)i = e^{F_1(x;T)=T} : \quad (1)$$

Here  $T rL(x)L^Y(0)$  is the trace of the product of two Polyakov lines at  $x$  and 0. The quark and the antiquark lines do not, in general, form a close loop. As a gauge transformation introduces phase factors at the beginning and the end of an open Polyakov line,  $hTrL(x)L^Y(0)i$  is not gauge invariant under a gauge transformation. Calculations have been carried out in the color-Coulomb gauge which is the proper gauge to study bound states.

It should be noted that while the interaction between the quark and the antiquark is gauge dependent, the bound state energies are physical quantities and they do not depend on the gauge. As we explain below, a judicious choice of the Coulomb gauge in the bound state calculation will help in avoiding spurious next-to-leading contributions and singularities, which can be removed in other gauges only by great effort [43, 44, 45].

To study the bound states of a heavy quarkonium, we need a bound-state equation, such as the Bethe-Salpeter equation, and the interaction kernel in the equation. The non-relativistic approximation of the Bethe-Salpeter equation leads to the usual Schrödinger equation with the gauge-boson-exchange interaction [46, 47]. It is necessary to choose a gauge to specify the gauge-boson-exchange interaction. We can consider the case of QED from which we can get a good insight on the gauge dependence. For the static non-relativistic problem, the natural choice in the gauge-boson-exchange potential is the Coulomb gauge, in which the  $1=Q^2$  behavior is found in single Coulomb photon exchange. The binding energy, which is of order  $1^2$ , has corrections only in the  $1^4$  order. It gives the correct Breit equation with the proper spin properties when we expand the interaction to the next order. Graphs with the cross two-Coulomb-exchange diagrams vanish in the static limit, and uncrossed multiple Coulomb exchanges are strictly iterations of the potential [43]. In any other gauge, the zero-zero component of the photon propagator has some residual non-instantaneous contributions. A large number of Bethe-Salpeter kernels need to be included to eliminate the spurious contributions in the next-order of  $1^3$  and  $1^3=\ln$  corrections [44, 45]. Therefore, in their work on the static potential in QCD, Appelquist, Dine, and Mizinich suggested that the gauge freedom can be used to eliminate spurious long-range forces at the outset. They found that the Coulomb gauge continues to be useful in examining the static potential in QCD. The dynamics is now considerably complicated but spurious contributions are still eliminated [43].

Based on the above, it is therefore important to recognize, as in QED, that there is a gauge-dependence in the two-body bound-state potential in the Bethe-Salpeter equation but it is most appropriate to solve the bound state problem using two-body potentials obtained in the Coulomb gauge, as was obtained by Kaczmarek et al [17].

### IV. COLOR-SINGLET Q-Q POTENTIAL

Kaczmarek et al: [17] calculated the color-singlet internal energy  $V_1(r;T)$  from the free energy  $F_1(r;T)$ ,

$$V_1(r;T) = F_1(r;T) - T \frac{\partial F_1(R;T)}{\partial T} : \quad (2)$$

We shall follow Zantov, Kaczmarek, Karsch and Petreczky in Ref. [25] to use the internal energy, rather than the free energy to model the potential. We can justify the use of the internal energy  $V_1(r;T)$  as follows.

We are interested in the effective energy between a quark and an antiquark (with their equilibrium gluon clouds) in a color-singlet state. When a quark and an antiquark are placed in the sea of gluons at a temperature  $T$  above  $T_c$

in equilibrium. The quark and antiquark in the lattice gauge calculations are each surrounded by a cloud of gluons. The clouds of gluons will interact with the bare quark and also with the bare antiquark which will lead to additional contributions to the interaction between the quark and the antiquark. These interactions, together with the bare interaction between the heavy quark and the heavy antiquark, constitute the effective interaction (internal energy) between the quark and the antiquark in the lattice gauge calculation.

However, as the separation between the quark and the antiquark changes, the potential experienced by the gluons also changes. The clouds of gluons in the field of the quark and the antiquark occupy different gluon states. These different gluon occupation probabilities contribute to the entropy and the free energy of the system (as given by the derivative of the free energy of the system with respect to the temperature). As the separation changes, these different gluon occupation probabilities lead to a change of the entropy and the total free energy as a function of the separation. It is necessary to subtract this contribution from the total free energy to obtain the effective interaction between the quark and the antiquark for bound state studies, as is carried out according to Eq. (2) in the procedures suggested by Zantow et al. [25]. Accordingly, the two-body wave function  $\psi(r;T)$  satisfies the Schrödinger equation

$$\frac{r^2}{2m_{\text{red}}} + [V_1(r;T) - V_1(r \rightarrow 1;T)]\psi(r;T) = E(T)\psi(r;T); \quad (3)$$

where  $m_{\text{red}} = m_Q m_{\bar{Q}} = (m_Q + m_{\bar{Q}})$  is the reduced mass of the interacting  $Q$  and  $\bar{Q}$ , and the eigenenergy  $E(T)$  is measured relative to the asymptotic potential at which  $Q$  and  $\bar{Q}$  are separated by an asymptotically large distance. The solution of the Schrödinger equation gives the eigenenergies and eigenfunctions of the heavy quarkonium system.

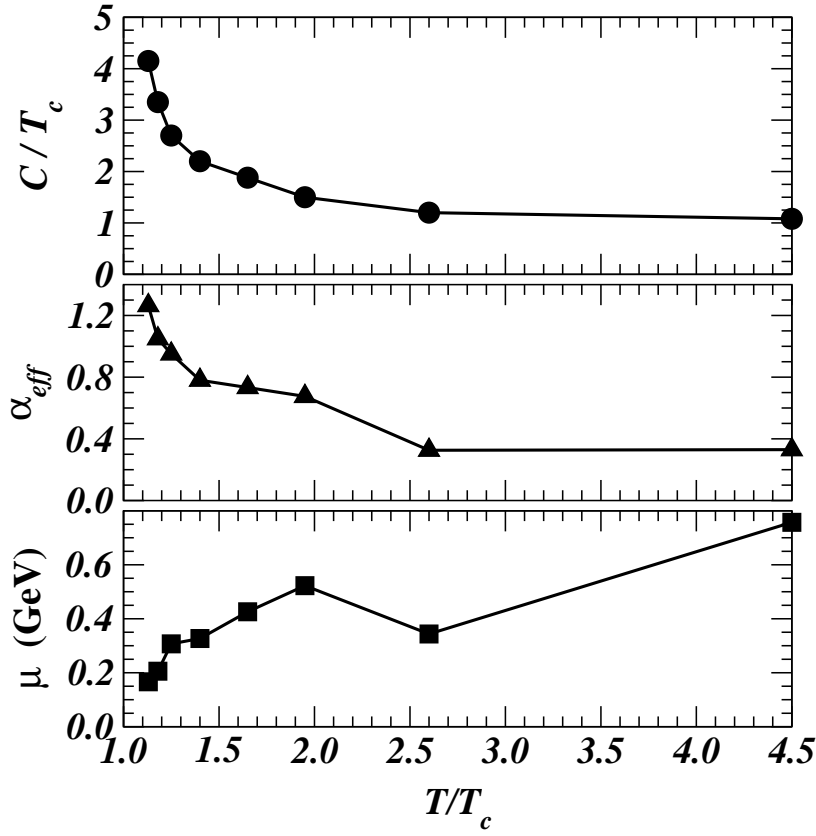


FIG. 1: Color-singlet heavy quarkonium potential parameters.

The color-singlet heavy-quark and antiquark potential  $V_1(r;T)$  in quenched QCD obtained by Kaczmarek et al. [17] can be adequately represented by a screened color-Coulomb potential with a screening mass  $\mu$ , an effective strong interaction coupling constant  $\alpha_{\text{eff}}$ , and an asymptotic potential horizon  $C(T)$  at  $r \rightarrow 1$ ,

$$V_1(r;T) = C(T) - \frac{4\pi\alpha_{\text{eff}}(T)}{3} \frac{e^{-\mu(T)r}}{r}; \quad (4)$$

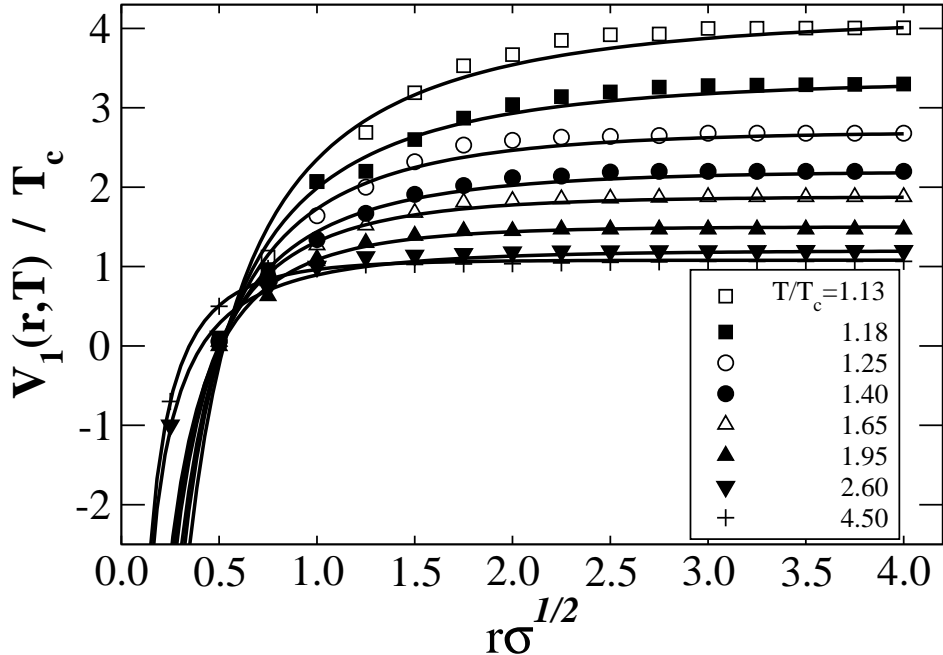


FIG. 2: The symbols represent the quenched lattice QCD potential,  $V_1(r;T) = T_c$ , of Kaczmarek et al: [17] at selected distances and the curves are fits using the screened color-Coulomb potential, Eq. (4), with parameters given in Fig. 1. Here  $\sigma^{1/2} = 425$  MeV.

The parameters  $C(T)$ ,  $\epsilon_e(T)$ , and  $\epsilon_s(T)$  can be obtained as a function of temperature by fitting the numerical quenched lattice QCD results  $V_1(r;T)$  of Kaczmarek et al: [17] with the potential of the above parameterized form. The values of the parameters as a function of the temperature are shown in Fig. 1, and the corresponding fits to the lattice results are shown in Fig. 2. The effective coupling constant  $\epsilon_e(T)$  is very large at temperatures slightly above the phase transition temperature. At  $T = 1.13 T_c$ ,  $\epsilon_e(T) = 1.26$ . As the temperature increases,  $\epsilon_e(T)$  decreases and saturates at  $\epsilon_e(T) \approx 0.4$  at  $T = 4T_c$ . The screening mass is small at temperatures just above  $T_c$ . For these temperatures, the Q-Q interaction is nearly a color-Coulomb interaction with a large coupling constant. The large gluon-quark coupling strength at temperatures slightly greater than  $T_c$  has been noted earlier by Karsch et al: [5] and has recently been emphasized by Gyulassy, McLerran, and Shuryak [13, 38, 39] in their discussions concerning the discoveries of the strongly interacting QGP (sQGP) at RHIC [13, 38]. As the temperature increases, the screening mass increases to about 0.8 GeV at  $T = 4T_c$ . The comparison in Fig. 2 shows that the screened color-Coulomb potential Eq. (4), with the set of parameters in Fig. 1, adequately describes the lattice-gauge data and can be used to calculate the eigenvalues and eigenfunctions of heavy quarkonia.

## V. ANTISCREENING BY DECONFINED GLUONS

In the conventional description, the Debye screening due to deconfined quarks and gluons is considered to be the dominant medium effect when a heavy quarkonium is placed in a quark-gluon plasma [1]. It is argued that Debye screening leads to a decrease in the attractive interaction between the heavy quark and antiquark and results in the spontaneous dissociation of the heavy quarkonium in the quark-gluon plasma. The suppression of  $J/\psi$  production was suggested as a signature for the quark-gluon plasma [1].

The potential parameters extracted from the lattice gauge calculations of Kaczmarek et al: [17] in the last section provide useful insight into the medium effects on the interaction between a heavy quark and a heavy antiquark. One can examine whether these potential parameters fit the picture of Debye screening as suggested by Matsui and Satz [1].

The parameter  $\epsilon_e$  in Fig. 1 is the strength of the quark-antiquark attractive color-Coulomb interaction in the color-singlet state in the quark-gluon plasma, and the parameter  $\epsilon_s$  is the corresponding screening mass. In perturbative QCD, there is a relation between the screening mass  $\sigma$ , coupling constant  $g = \frac{1}{4\pi} \frac{1}{\epsilon_s}$  and temperature

$T$  in a quark-gluon plasma a given by [48, 49, 50, 51, 52]

$$^2 = g^2 T^2 (N_c + N_f) = 3: \quad (5)$$

For the quenched approximation with  $N_f = 0$ , perturbative QCD gives  $= gT$ . We can compare this perturbative QCD result with those from the lattice gauge calculations of Kaczmarek et al: [17] by identifying  $\epsilon$  of Fig. 1 as the strong coupling constant  $s$ . We plot the quantity  $= gT$  as a function of  $T = T_c$  in Fig. 3 where the transition temperature  $T_c$  is equal to 269 MeV in the quenched approximation [5]. The comparison in Fig. 3 shows that the

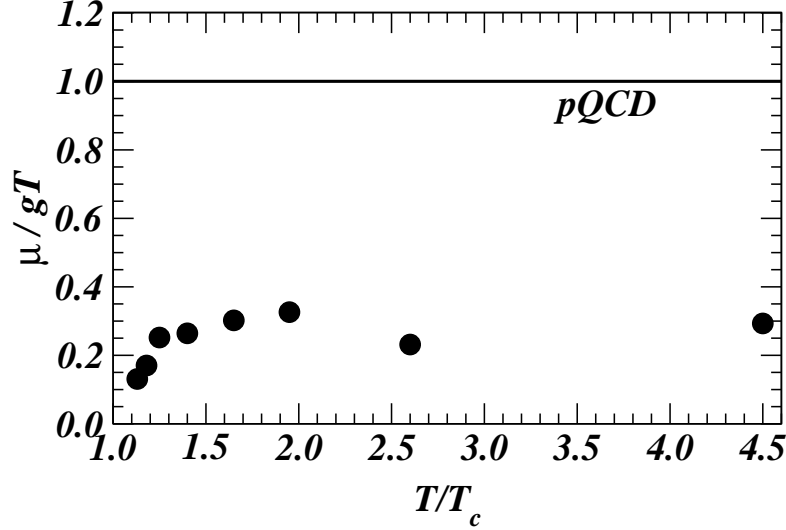


FIG. 3: The ratio of  $= gT$  extracted from the lattice calculations as compared with the perturbative predictions of  $= gT = 1$ .

ratio  $= gT$  from the lattice gauge calculations of Kaczmarek et al: [17] differs significantly from the perturbative QCD result of  $= gT = 1$ . As is well known, screening effects are highly non-perturbative in the region of temperatures slightly above  $T_c$  [53]. The results in Fig. 3 represent another example of the non-perturbative behavior.

When one looks carefully at the results of Figs. 1 and 3, one notes that at temperatures above  $1.5T_c$ , the ratio  $= gT$  reaches a plateau value, as in the results of perturbative QCD. However, the plateau value of the ratios  $= gT$  is substantially smaller than what is expected from perturbative QCD. Furthermore, the screening mass  $m$  approaches zero at  $T = T_c$ . At the same time, the effective coupling constant  $\epsilon$  is very large. It is of the order of unity, much larger than the coupling constant between a heavy quark and antiquark in free space. These peculiar features suggest that in addition to the Debye screening, there is a mechanism that is important in mediating the interaction between a heavy quark and antiquark. It is of great interest to understand the physical origin of this counterbalancing mechanism just above  $T_c$ . Specifically, one looks for a mechanism that

1. counterbalances and overwhelms the effects of screening at  $T$  just above  $T_c$ ,
2. enhances the attractive interaction between the heavy quark and the antiquark, especially at  $T$  just above  $T_c$ ,
3. suppresses the effects of screening substantially at higher temperatures ( $1.5 < T = T_c < 4.5$  in Fig. 3), and
4. becomes operational when  $T$  exceeds  $T_c$ .

The most probable mechanism that possesses these features appears to be the mechanism of antiscreening by deconfined gluons.

The mechanism of antiscreening by virtual gluons at  $T = 0$  is well known (see for example [54, 55]). As one crosses the phase transition temperature  $T_c$  from below, the medium changes from a hadronic matter to a quark-gluon plasma. Quarks and gluons becomes deconfined and will be the quanta of the medium. The medium effects of deconfined gluons becomes abruptly more important, when a heavy quarkonium is placed in the medium just above the phase transition temperature. While deconfined gluons can screen the  $Q\bar{Q}$  interaction, it can also antiscreen the  $Q\bar{Q}$  interaction.

To study how a gluon medium can affect the interaction between the heavy quark and antiquark, we shall represent the deconfined gluons in terms of an external gluon field  $A^{bi}(r)$  where the first index  $b = 1, \dots, 8$  is the color index, and the second index  $i = 1, 2, 3$  is the spatial coordinate index. We need to fix a gauge and we shall use the Coulomb

gauge which is the most convenient gauge for quarkonium bound state calculations (see Section III). We would like to show that because the Gauss law of QCD contains a non-linear term involving the gauge field  $A^{bi}$ , the gluon field induces color charges at the field points between the heavy quark and antiquark. These induced color charges act to antiscreen the interaction between the heavy quark and the antiquark. We shall show that the strength of the antiscreening effect increases with the correlation length and is proportional quadratically to the magnitude of the gluon field which increases with the density of deconfined gluons. As the correlation length is very large and the density of deconfined gluons increases copiously when the temperature exceeds the phase transition temperature, the antiscreening effects due to deconfined gluons brings a new degree of freedom to mediate the interaction between the quark and the antiquark. It is tempting to suggest that the antiscreening due to the presence of a large number of deconfined gluons in the medium at the onset of the phase transition counterbalances the effects of screening and enhances the attractive interaction between the heavy quark and antiquark at  $T$  slightly greater than  $T_c$ .

It will be difficult to quantify the effects of antiscreening in a nonperturbative treatment. It suffices to spell out the perturbative origin of the antiscreening effect due to external gluon fields. We shall follow arguments similar to those presented by Peskin, Gottfried, and Weisskopf [54, 55] in their discussions on the analogous case of antiscreening effects due to virtual gluons at  $T = 0$ .

We study the color electric field generated by a static color source  $\mathbf{a}^{(0)}_{ext}(\mathbf{r}) = (r)^a$  with a unit color charge of index placed at the origin, in the presence of an external gauge field  $A^{bi}(\mathbf{r})$ . The color electric field  $E^{ai}(\mathbf{r})$  generated by this source is determined by the Gauss law

$$\partial_i E^{ai}(\mathbf{r}) = g (r)^a + g f^{abc} A^{bi}(\mathbf{r}) E^{ci}(\mathbf{r}) \quad (6)$$

(Eq. (16.139) of Peskin and Schroeder [55]). Here repeated indices are summed over and the first index of  $E^{ai}(\mathbf{r})$  is the color index and the second index is the spatial coordinate index. Because of the non-linear nature of the second term which arises from the non-Abelian nature of QCD, the external color source  $(r)^a$  and the external gauge field  $A^{ai}(\mathbf{r})$  induce a color source  $\mathbf{a}^{(1)}_{ind}(\mathbf{r})$ , which in turn induces an additional color source  $\mathbf{a}^{(2)}_{ind}(\mathbf{r})$ . How does these induced color charge depend on the external gauge field  $A^{bi}(\mathbf{r})$ ?

We consider an expansion of the source in terms of the external source and the induced sources, in powers of the coupling constant

$$\partial_i E^{ai}(\mathbf{r}) = g (x)^a + g \mathbf{a}^{(1)}_{ind}(\mathbf{r}) + g \mathbf{a}^{(2)}_{ind}(\mathbf{r}) + \dots \quad (7)$$

In the Coulomb gauge, the color field  $E^{ci(1)}(\mathbf{r})$ , as arising only from the external static source  $(r)^a$ , is

$$E^{ci(1)}(\mathbf{r}) = g^a \frac{r^i}{r^3} : \quad (8)$$

From the non-linear term in Eq. (6), the color charge density induced at  $\mathbf{r}$  by the external gauge field  $A^{bi}(\mathbf{r})$  and the electric field  $E^{ci(1)}(\mathbf{r})$  of the external color source is

$$\mathbf{a}^{(1)}_{ind}(\mathbf{r}) = f^a A^i(\mathbf{r}) E^{ci(1)}(\mathbf{r}) = g f^a A^i(\mathbf{r}) \frac{r^i}{r^3} : \quad (9)$$

An induced color-charge element  $\mathbf{a}^{(1)}_{ind}(\mathbf{r}) \mathbf{r}$  at  $\mathbf{r}$  will generate a field  $E^{ai(2)}(\mathbf{r}^0; \mathbf{r})$  at  $\mathbf{r}^0$  and this field is pointing along the direction of  $\mathbf{r}^0 - \mathbf{r}$ ,

$$E^{ai(2)}(\mathbf{r}^0; \mathbf{r}) = g [\mathbf{a}^{(1)}_{ind}(\mathbf{r}) \mathbf{r}] \frac{(r^{0i} - r^i)}{r^0 r^3} : \quad (10)$$

From the non-linear term in Eq. (6), the color charge density element  $\mathbf{a}^{(2)}_{ind}(\mathbf{r}^0; \mathbf{r}) \mathbf{r}$ , that is induced at  $\mathbf{r}^0$  by the external gauge field  $A^{bi}(\mathbf{r}^0)$  and the electric field  $E^{ci(2)}(\mathbf{r}^0; \mathbf{r})$  at  $\mathbf{r}^0$ , is therefore

$$\mathbf{a}^{(2)}_{ind}(\mathbf{r}^0; \mathbf{r}) \mathbf{r} = f^{abc} A^{bi}(\mathbf{r}^0) E^{ci(2)}(\mathbf{r}^0; \mathbf{r}) = g^2 f^{abc} A^{bi}(\mathbf{r}^0) f^c A^j(\mathbf{r}) \frac{r^j}{r^0 r^3} \mathbf{r} \cdot \frac{(r^{0i} - r^i)}{r^0 r^3} : \quad (11)$$

As the external source has the color index  $a$ , we would like to study the induced color charge of index  $a$  to see whether the induced color charges lead to screening or antiscreening. From Eq. (9), we have

$$\mathbf{a}^{(1)}_{ind}(\mathbf{r}) = 0; \quad (12)$$

as  $f_{\text{ind}}^{(2)}(r^0; r) = 0$  on account of the antisymmetric property of  $f$ . For the next order induced color charge density element  $f_{\text{ind}}^{(2)}(r^0; r)$ , we can write out explicitly the summations of color and spatial indices of Eq. (11),

$$f_{\text{ind}}^{(2)}(r^0; r) = g^2 \sum_{b;c=1}^{X^8} f^{bc} f^c = \sum_{i;j=1}^{X^3} \frac{A^{bi}(r^0) (r^{0i} - r^i) A^{bj}(r) r^j}{r^3 r^0 r^3} r^0 : \quad (13)$$

We note that

$$f^{bc} f^c = F( ; b) \quad (14)$$

where  $F( ; b)$  is a non-negative quantity defined by

$$F( ; b) = \sum_{c=1}^{X^8} (f^{bc})^2, \quad (15)$$

which can be easily evaluated. For example,  $F(1; b)$  is  $f(0; 1; 1; 1; 1=4; 1=4; 1=4; 1=4; 0g$  for  $b = 1; 2; \dots; 8$ . In terms of  $F( ; b)$ , the induced charge density is

$$f_{\text{ind}}^{(2)}(r^0; r) = g^2 \sum_{b=1}^{X^8} F( ; b) r^0 \sum_{i;j=1}^{X^3} \frac{A^{bi}(r^0) A^{bj}(r) (r^{0i} - r^i) r^j}{r^3 r^0 r^3} : \quad (16)$$

Note that  $F( ; ) = 0$ . The contribution of the external gauge field to the sum over  $b$  comes only from those color

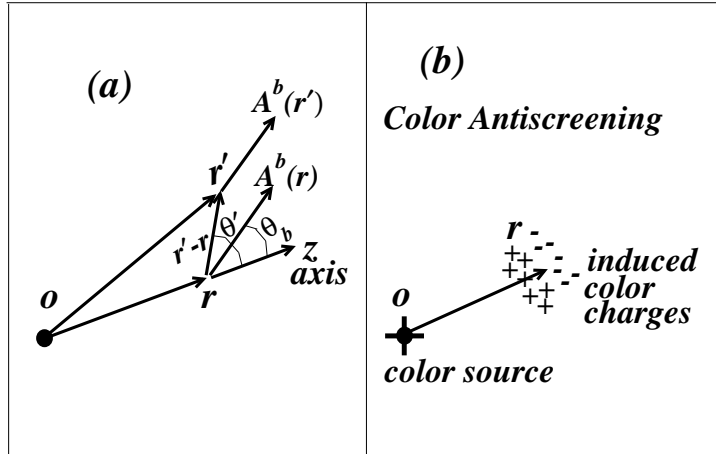


FIG. 4: (a) The coordinate system used in the evaluation of the induced color charge density  $f_{\text{ind}}^{(2)}(r^0; r)$  at  $r^0$ . (b) A heavy quark of color source at  $o$  induces color charges of the same sign in the direction forward of  $r$  and color charges of the opposite sign in the direction backward of  $r$ .

components of  $A^{bi}$  that are transverse to the color axis of the external point source.

The product  $A^{bi}(r^0) A^{bj}(r)$  in Eq. (16) involves spatial gauge fields at different spatial locations. Previously, Svetitsky, Yaffe, Detar and DeGrand found that large space-like Wilson loops in the quark-gluon plasma have an area law behavior. Such a behavior indicates that the spatial gauge fields  $A^{bj}(r)$  at different spatial locations are correlated [2, 3, 56, 57, 58]. We can express the thermal average of the  $A^{bi}(r^0) A^{bj}(r)$  in terms of the relative coordinate coordinate and the correlation length  $\zeta$ ,

$$\langle A^{bi}(r^0) A^{bj}(r) \rangle = \langle A^{bi}(r) A^{bj}(r) \rangle e^{-\frac{|r^0 - r|}{\zeta}} : \quad (17)$$

The quenched QCD calculations in  $SU(3)$  is in the universal class of three dimensional  $Z(3)$  symmetry. It has a first order phase transition and a large but finite correlation length at  $T_c$  [2, 3, 56, 57, 58, 59, 60, 61, 62, 63].

To study the sign of the induced color charges, we choose a spatial coordinate system with the  $z$ -axis along  $r$  as shown in Fig. (4a). In this coordinate system, we label the angular coordinates of  $r^0 - r$  and  $A^b(r)$  by  $(\theta^0, \theta^b)$  and

( $b$ ;  $b$ ), respectively. We shall study the induced charge at  $r^0$  within the correlation length of  $r$ . Then, after taking the thermal average, the induced color charge density is then

$$\text{ind}^{(2)}(r^0; r) = g^2 \sum_{b=1}^{X^8} F(b; b) r \frac{\bar{A}^b(r)^2 e^{\frac{r^0 - r^b}{r^2}}}{r^2 r^0 r^b} \cos_b [\cos_b \cos^0 + \sin_b \sin^0 \cos(\phi_b - \phi^0)]; \quad (18)$$

If we average over the azimuthal angle  $\phi^0$ , the second term in the square bracket drops out and we have

$$\text{ind}^{(2)}(r^0; r) = g^2 \sum_{b=1}^{X^8} F(b; b) r \frac{\bar{A}^b(r)^2 \cos^2_b e^{\frac{r^0 - r^b}{r^2}} \cos^0}{r^2 (r^2 + r^0 r^b + 2r^0 r^b \cos^0)}; \quad (19)$$

One readily observes that the induced color charge density  $\text{ind}^{(2)}(r^0; r)$  at  $r^0$  is negative in the forward hemisphere in the direction forward of  $r$  (with  $\phi^0 = 0$ ). It changes to positive in the backward hemisphere, in the direction backward of  $r$  ( $\phi^0 = \pi/2$ ). In the region of  $r^0$  within the correlation length from  $r$ , the induced charge surrounding  $r$  is a color-dipole type density distribution with the color charge of the same sign at distances closer to the color source and of the opposite sign at distances farther to the color source (Fig. 4b). This is the antiscreening behavior due to the presence of external gauge field  $\bar{A}^b(r)$  at  $r$ . The magnitude of the induced color charges will increase with an increase in the correlation length and the magnitude of the gluon field. The antiscreening effects will enhance the attractive interaction between the heavy quark and antiquark and will reduce the screening mass from the Debye screening predictions.

At the onset of the phase transition, the correlation length is very large [2, 3, 56, 57, 58, 59, 60, 61, 62, 63, 64, 65] and there is furthermore an abrupt increase in the number of deconfined gluons (or equivalently the strength of the gluon field  $\bar{A}^b(r)$ ), giving rise to a very strong antiscreening effect. The antiscreening effects due to deconfined gluons may be responsible for counterbalancing and overwhelming the effects of Debye screening and may lead a strong attractive coupling between the heavy quark and antiquark and the nearly zero screening mass at  $T = T_c$  as shown in Fig. 1.

At a higher temperature, a greater thermal fluctuation leads to a smaller correlation length and reduces the effects of antiscreening. However a high temperature is also accompanied by a greater gluon density which enhances the effects of antiscreening. The suppression of the ratio  $=gT$  from the PQCD behavior shown in Fig. 3 may be interpreted as due to the counterbalancing of the antiscreening of deconfined gluons against Debye screening. The effects of antiscreening appears to remain quite strong even at temperatures of  $T = 4.5T_c$ .

We can try to understand the peculiar behavior of the large value of  $C(T)$  near  $T_c$  in the lattice gauge results shown in Fig. 1. The quantity  $C(T)$  is the value of the  $Q\bar{Q}$  potential at large separations, when the potential is normalized to be approximately the same at short distances for all temperatures [17]. As we explained above, the effects of antiscreening are stronger at  $T = T_c$  than at higher temperatures. Such a difference has two main consequences. First, as one moves the heavy antiquark  $Q$  to greater and greater distances away from the heavy quark  $Q$ , the stronger antiscreening effect at  $T = T_c$  will make the heavy antiquark experience a greater amount of induced color charges of the same color as the heavy quark color charge. Thus the heavy antiquark at large separations sees a deeper and deeper potential. In the quark-gluon plasma, this increase in potential depth will reach a constant value until any further increases in the separation of  $Q$  and  $Q$  will not change the interaction between them. One expects that relative to the potential at large separations, the potential well at the origin is deeper at  $T = T_c$  than at higher temperatures. Second, even at large separations, the isolated heavy quark (and the heavy antiquark) each will be surrounded by greater induced color charges of the same kind at  $T = T_c$  than at higher temperatures. The energy of the isolated heavy quark and antiquark at large separations will also be greater. Therefore, when we normalize the  $Q\bar{Q}$  potential at different temperatures by its values at  $r = 0$ , we need to raise the energy at large separations at  $T = T_c$  because of these two effects of a greater potential depth and greater induced color charges surrounding the isolated quark and antiquark. As a result, there is a substantial enhancement of  $C(T)$  at  $T = T_c$  compared to the region at higher temperatures, as shown in Fig. 1.

## VI. CHARMONIUM IN QUARK-GLUON PLASMA

In the quenched approximation, the transition temperature is  $T_c = 269$  MeV [5]. We use this value of  $T_c$  to express the potential  $V_1(r; T)$  in GeV units, in order to evaluate the energy levels of different heavy quarkonia.

For a given temperature, the screened color-Coulomb potential with parameters given in Fig. 1 is used to calculate the charmonium energy levels and wave functions. In these calculations, we employ a charm quark mass  $m_c = 1.3$

GeV which lies within the charm quark mass range of 1.0–1.4 GeV in the PDG listing [66]. The use of different  $m_c$  values will modify the binding energy and the dissociation temperature slightly. For example, near the dissociation temperature, the binding energy of  $J/\psi$  at  $T = 1.95 T_c$  is 0.0135 GeV for  $m_c = 1.3$  GeV and is 0.0311 GeV for  $m_c = 1.5$  GeV.

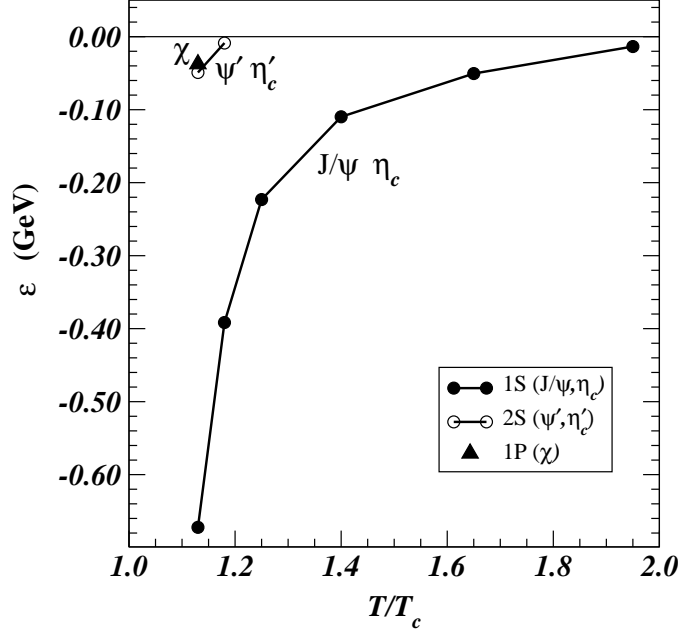


FIG. 5: Energy levels of charm onium in the quark-gluon plasma as a function of temperature.

Energy levels of charm onium in the quark-gluon plasma as a function of temperature are shown in Fig. 5. We note that the eigenenergies of  $J/\psi$  and  $\eta_c$  are about -0.7 GeV at  $T = 1.1 T_c$  and they increase as the temperature increases. The  $J/\psi$  state eigenenergy is -0.0135 GeV at  $T = 1.95 T_c$ , and it is unbound at  $T = 2.6 T_c$ . One can define the spontaneous dissociation temperature of a heavy quarkonium as the temperature at which the quarkonium begins to be unbound and dissociates spontaneously. The  $J/\psi$  spontaneous dissociation temperature lies between  $1.95 T_c$  and  $2.6 T_c$ . If one extrapolates the eigenenergy from lower temperature points, one infers the  $J/\psi$  spontaneous dissociation temperature to be about  $2 T_c$ .

Because the screening mass is small at temperatures slightly above  $T_c$  the  $Q\bar{Q}$  potential is nearly a color-Coulomb potential with nearly degenerate 1P and 2S states at these temperatures. The nearly degenerate  $\chi$ ,  $\psi'$ , and  $\eta_c$  states begin to be unbound at  $T = 1.2 T_c$ .

In the spectral analyses of Asakawa et al: [6, 7] and Petreczky et al: [8, 9, 10], the widths of  $J/\psi$  and  $\eta_c$  begin to be broadened at  $1.6 T_c$  and  $1.1 T_c$  respectively. If we associate the broadening of the widths of heavy quarkonia in the spectral analysis with the occurrence of dissociation, the temperatures at which the widths of the quarkonium begin to broaden can be taken as the dissociation temperatures in that analysis.

In Table I we list the dissociation temperatures of different quarkonia obtained in quenched QCD. A comparison of the dissociation temperatures in the spectral analysis [6, 7, 8, 9, 10] and in the present potential model analysis indicates qualitative agreement that  $J/\psi$  and  $\eta_c$  are stable at temperatures slightly above  $T_c$  and are unstable at very high temperatures. They differ quantitatively, however, at the locations of the dissociation temperatures. The dissociation temperatures differ by  $0.4 T_c$  for  $J/\psi$  and  $0.1 T_c$  for  $\eta_c$ .

It is worth pointing out that the dissociation temperatures in the potential model analysis refer to those of spontaneous dissociation. In the spectral analysis, on the other hand, the width of a heavy quarkonium includes the width for spontaneous dissociation and presumably also the width due to the dissociation of the heavy quarkonium in its interaction (or collision) with gluons. Because of this additional mode of dissociation, it is reasonable that the widths of  $J/\psi$  and  $\eta_c$  in the spectral analysis begin to be broadened at temperatures lower than their corresponding spontaneous dissociation temperatures. We shall study the width of dissociation due to the collision of  $J/\psi$  with gluons in the potential model in Section IX.

There are uncertainties in the spontaneous dissociation temperatures due to the differences in the degrees of freedom assumed in lattice QCD calculations. For example, using the  $Q\bar{Q}$  potential extracted from the full QCD with two flavors obtained by Kaczmarek et al: [67], Shuryak found that the dissociation temperature of  $J/\psi$  is about  $2.7 T_c$  [12].

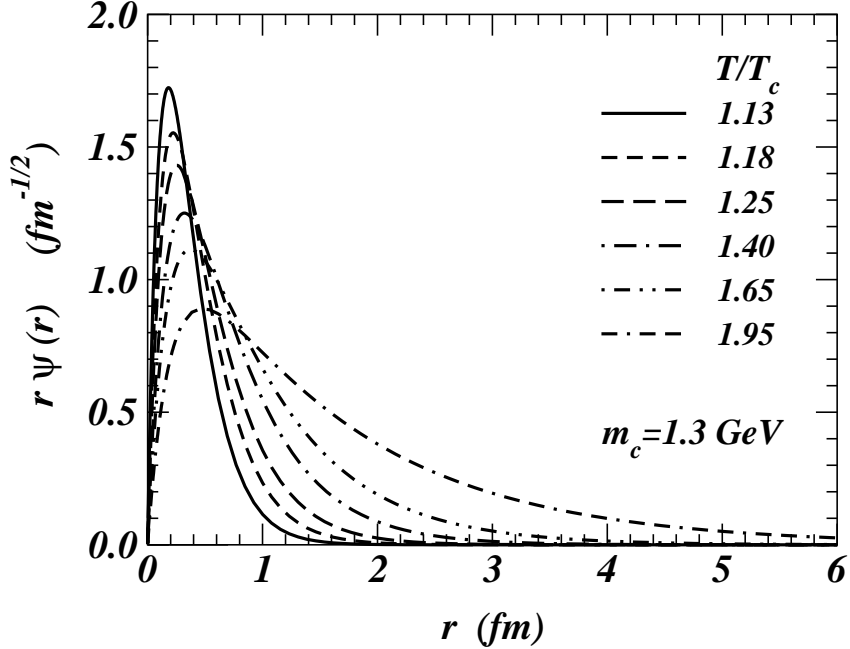
FIG. 6:  $J=1/2$  wave function as a function of temperature.

Table I. Dissociation temperatures obtained from different analyses in quenched QCD.

Heavy Quarkonium	Potential Model Spontaneous Dissociation Temperature	Spectral Analysis Dissociation Temperature
$J/\psi_c$	$2T_c$	$1.6T_c$
$c\bar{c}; \psi_c^0$	$1.2T_c$	$1.1T_c$
$J/\psi_b$	$4.5T_c$	
$b\bar{b}; \psi_b^0$	$2T_c$	

The solution of the Schrodinger equation (3) gives both eigenenergies and eigenfunctions. We show in Fig. 6 the wave functions of  $J=1/2$  which are normalized according to

$$\int_0^{Z_1} j_{1s}(r) \frac{dr}{r} = \int_0^{Z_1} j_{1s}(r) \frac{dr}{r} = 1; \quad (20)$$

as in Eq. (4.18) of Biall and Weisskopf [71]. As the temperature increases, the binding of the state becomes weaker and the wave function extends farther out to greater distances. At  $T = 1.90T_c$ , which is near the temperature for spontaneous dissociation, the rms radius of the  $J=1/2$  wave function is 1.30 fm, which is much greater than the theoretical rms radius of 0.404 fm for  $J=1/2$  at zero temperature [68].

## VII. (b) BOUND STATES IN QUARK-GLUON PLASMA

One can carry out similar calculations for the energy levels and wave functions of the  $b\bar{b}$  system. We take the mass of the bottom quark to be 4.3 GeV, which falls within the range of 4.1 to 4.5 GeV in the PDG listing [66]. The energy levels of the lowest  $b\bar{b}$  bound states as a function of temperature are shown in Fig. 7. We find that at  $T = 1.13T_c$ , the state lies at -2.8 GeV and the state energy increases as the temperature increases, but the increase becomes very slow for  $T > 2.6T_c$ . The state remains to be bound by 0.017 GeV at  $T = 4.5T_c$ . The small binding energy at  $T = 4.5T_c$  indicates that the dissociation temperature is close to and slightly greater than  $T = 4.5T_c$ .

Because of the small screening mass, the potential for temperatures near  $T_c$  is approximately a color-Coulomb potential but with a large coupling constant. Hence, the  $1P$  and  $2S$  states are nearly degenerate. They lie at -0.5 GeV for  $T = 1.13T_c$ , and begin to be unbound at  $T = 2T_c$ .

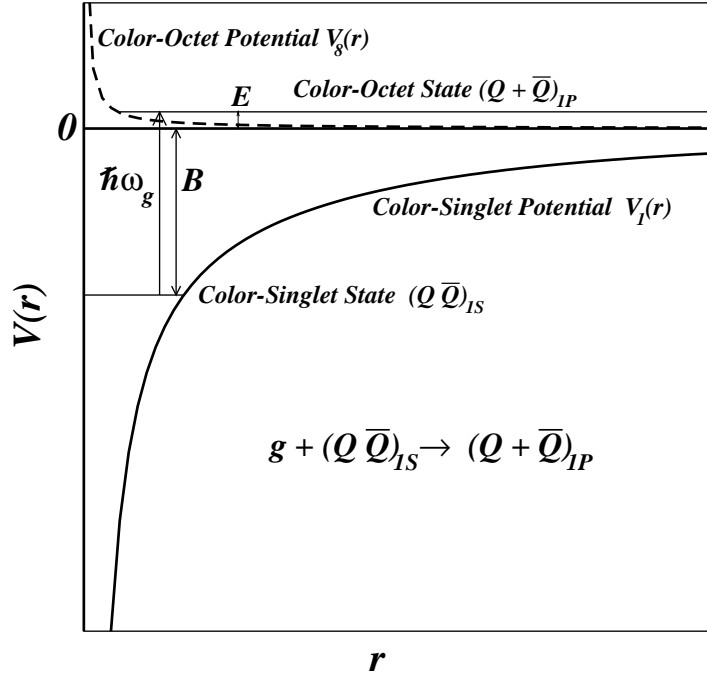


FIG . 7: Energy levels of (bb) bound states as a function of temperature.

The (bb) bound state wave functions can be obtained by solving the Schrodinger equation (3). We show in Fig. 8 the radial wave functions as a function of temperature. The wave function extends to greater distances as the temperature increases. At  $T = 4.5 T_c$ , which lies very close to the temperature for spontaneous dissociation, the rms value is 0.674 fm which is substantially greater than the theoretical rms of 0.255 fm at  $T = 0$ .

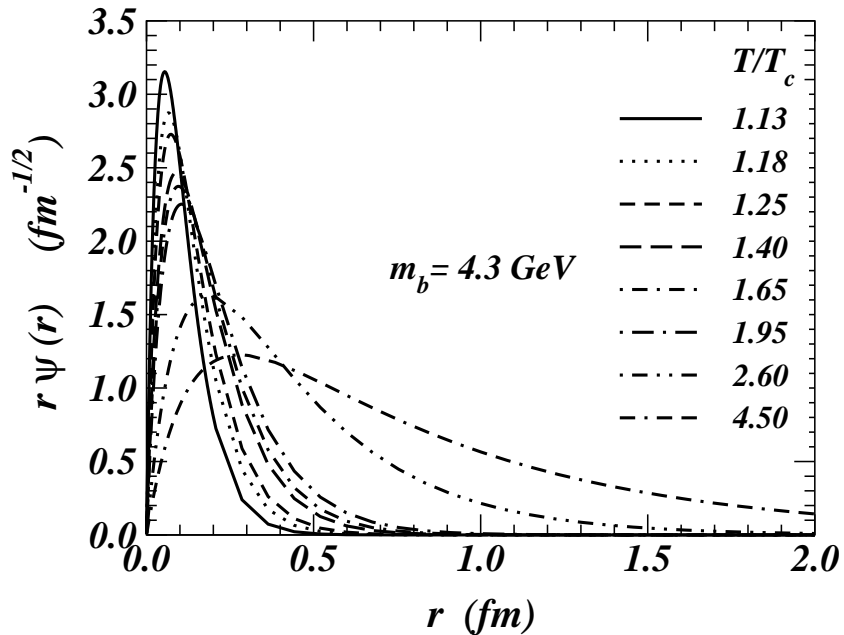


FIG . 8: wave function  $r \psi(r)$  as a function of temperature.

## V III. DISSOCIATION OF J= IN COLLISION WITH GLUONS

It is not necessary to reach the spontaneous dissociation temperature with zero binding energy for a quarkonium to dissociate. In a quark-gluon plasma, gluons and quarks can collide with a color-singlet heavy quarkonium to lead to the dissociation of the heavy quarkonium. Dissociation by the absorption of a single gluon is allowed as the color-octet final state of a free quark and a free antiquark can propagate in the color medium, in contrast to the situation below  $T_c$  in which the quark and the antiquark are confined. We shall consider dissociation of heavy quarkonium by gluons in the present work. The collision of a heavy quarkonium with light quarks can also lead to the dissociation of the heavy quarkonium, but through higher-order processes. They can be considered in future refined treatment of the dissociation process.

Previous treatment of the dissociation of heavy quarkonium by the absorption of a gluon was carried out by Peskin and Bhanot [69, 70]. They use the operator product expansion and the large  $N_c$  limit. They sum over a large set of diagrams and show that to obtain gauge invariant results, they need to sum over diagrams in which the external gluon is coupled to the gluon that is exchanged between the heavy quark and the heavy antiquark. They use hydrogen wave function and hydrogen states to evaluate the transition matrix elements. Their expression for the dissociation cross section of  $(g + (Q\bar{Q})_{1S} \rightarrow Q + \bar{Q})$  is

$$(g + (Q\bar{Q})_{1S} \rightarrow Q + \bar{Q}) = \frac{2}{3} \frac{32}{3}^2 \frac{4}{3^2 s} \frac{1}{m_Q^2} \frac{(E=B)^{3=2}}{(E=B+1)^5}; \quad (21)$$

where  $E$  is the non-relativistic kinetic energy of the dissociated  $Q$  and  $\bar{Q}$  in the center-of-mass system. In this short-distance approach of Peskin and Bhanot, the quark and the antiquark form a color-dipole pair and the gluons couple to the Wilson loop (the quarkonium) via simple dipole interactions. The dissociation cross section of Eq. (21) is, in fact, the dissociation of the quarkonium through the absorption of an E1 gluon radiation.

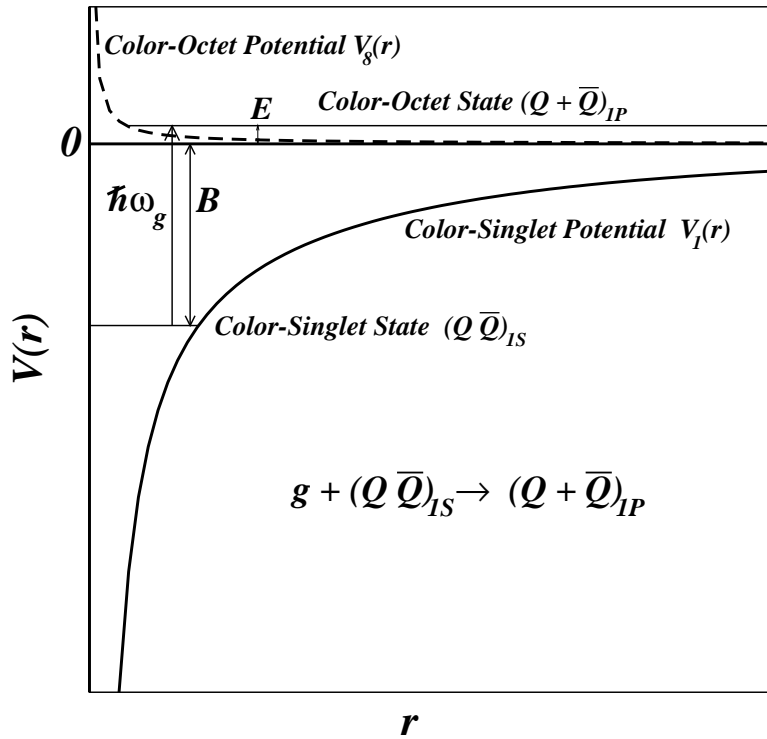


FIG. 9: The quarkonium dissociation process in the potential model.

Peskin and Bhanot's analytical result for the dissociation cross section has been applied to many calculations [21, 22, 72]. In heavy quarkonia of interest, the radial dependence of the quark-antiquark potential often differ from the Coulomb potential. The calculation of the dissociation cross section requires a new formulation which can be best described by the potential model introduced previously [20, 42], following the results of Bhatt and Weisskopf [71] obtained for the photo-disintegration of a deuteron. The dissociation process is schematically illustrated in Fig.

9. An initial bound  $(Q\bar{Q})_{1S}$  state with a binding energy  $B$  in the color-singlet potential  $V_1(r)$  absorbs a gluon of energy  $\sim !_g$ , and is excited to the color-octet final state  $(Q + \bar{Q})_{1P}$  with a kinetic energy  $E$  above the rest mass of  $m_Q + m_{\bar{Q}}$ . The interaction  $V_8(r)$  between  $Q$  and  $\bar{Q}$  in the color-octet state will be different from the interaction  $V_1(r)$  in the color-singlet state, as shown in Fig. 9. At low energies, the dominant dissociation cross section is the  $E1$  color-electric dipole transition for which the final state of  $Q + \bar{Q}$  will be in the  $1P$  state. The dissociation cross section ( $g + J= 1$   $c + c$ ) for such a color  $E1$  transition can be obtained from the analogous result in QED [20, 71], and the result is [20]

$$\frac{E_{\text{dis}}^1(E_{\text{gluon}})}{3} = 4 \frac{g_Q}{3} (k^2 + l^2) k^{-1} I^2; \quad (22)$$

where

$$E_{\text{gluon}} = B + E; \quad l^2 = 2B; \quad k^2 = 2E; \quad (23)$$

$$I = \int_0^{Z_1} u_{1P}(r) r u_{1S}(r) dr; \quad (24)$$

$$g_Q = s \frac{1}{2} 8c \frac{1}{2} \frac{1}{2} = s \frac{1}{6}; \quad (25)$$

and  $s$  is the gluon-(heavy quark) coupling leading to the dissociation of the heavy quarkonium. Here, we use the same notation and normalization as in Blatt and Weisskopf. The bound state wave function  $u_{1S}$  has been normalized according to Eq. (20) as in Eq. (XII.4.18) of Blatt and Weisskopf [71], and the continuum wave function  $u_{1P}$  is normalized according to

$$u_{1P}(r) \propto \frac{\sin(kr)}{kr} \quad \text{for } r \gg 1; \quad (26)$$

as in Eq. (XII.4.32) of Blatt and Weisskopf [71]. The result from the potential model agrees with the analytical results of Bhanot and Peskin for the case they considered (hydrogen wave function, large  $N_c$  limit, ... [20]). Such an agreement was further confirmed by numerical calculations according to Eq. (22) using hydrogen wave function for  $u_{1S}$  and plane wave continuum wave function for  $u_{1P}$ , as assumed by Peskin and Bhanot [69, 70]. The potential model has the practical advantage that it can be used for a  $Q\bar{Q}$  system with a general potential.

## IX. J=1 COLLISIONAL DISASSOCIATION RATE AND DISASSOCIATION WIDTH

We have represented the color-singlet potential between a heavy quark and antiquark by a screened color-Coulomb potential and have obtained the  $J=1$  wave function. To study the gluon dissociation of  $J=1$ , we need the color-octet potential  $V_8(r; T)$  experienced by the  $Q$  and  $\bar{Q}$  in the final state. We shall assume the generalization that the color-dependence of the potential Eq. (4) is simply obtained by modifying the color factor from  $4=3$  for the color-singlet state to  $1=6$  for the color-octet state:

$$V(r; T) = C(T) + C_f \frac{e(T) e^{-(T)r}}{r}; \quad (27)$$

$$C_f = \begin{cases} 4=3 & \text{(color singlet)} \\ 1=6 & \text{(color octet)} \end{cases} \quad (28)$$

We also need the gluon-quark coupling constant  $s$  in Eq. (25) to evaluate the dissociation cross section. We shall consider the screened color-Coulomb potential (22) obtained in the lattice-gauge theory as arising from the exchange of a virtual nonperturbative gluon. In such a viewpoint, the quantity  $e(T)$  in the screened color-Coulomb potential (4) for bound states is the gluon-(heavy quark) coupling constant  $s$  in the gluon-(heavy quark) interaction in Eq. (25) for dissociation. In other words, we assume that the coupling of gluon to the heavy quark leading to quarkonium bound states is the same coupling leading to the dissociation of the quarkonium. Thus,  $e(T)$  can be identified as  $s$  for the investigation of  $J=1$  dissociation. As  $e(T)$  is very large at temperatures just above the transition temperature  $T_c$  (Fig. 1), the gluon-(heavy quark) coupling is very strong at these temperatures, as was emphasized recently by Gyulassy, McLerran, and Shuryak [13, 38, 39], and discussed earlier by Karsch et al. [5]. With the above

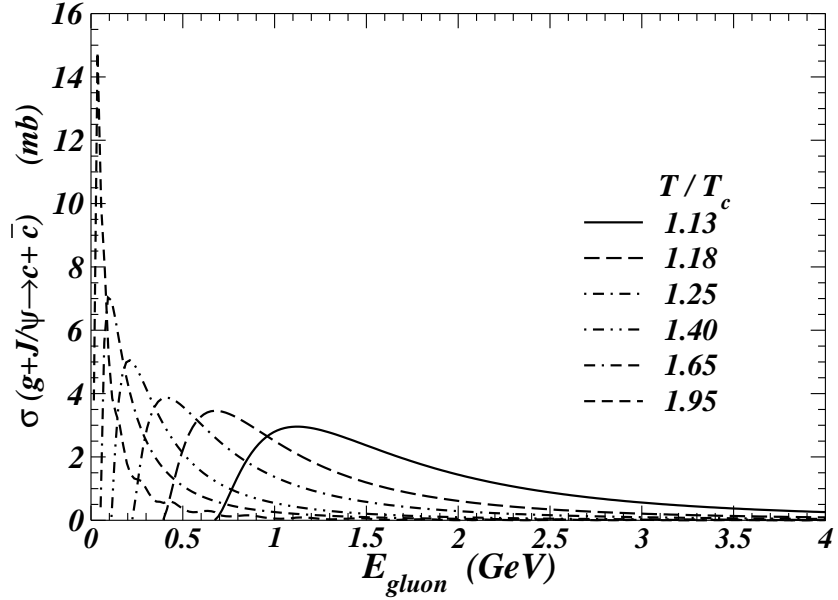


FIG. 10:  $J/\psi$  dissociation cross section as a function of gluon energy at various quark-gluon plasma temperatures.

additional information on various physical quantities of interest, the  $J/\psi$  dissociation cross section can be calculated using Eq. (22). The results of the  $J/\psi$  dissociation cross section for different temperatures are shown in Fig. 10. The cross section increases up to a maximum value and decreases as the gluon energy increases. The maximum height of the dissociation cross section increases, but the width of the cross section decreases as the temperature increases. We shall limit our attention to the dissociation of  $J/\psi$  by the absorption of an E1 radiation in the present analysis. When the dissociation threshold decreases, higher multipole dissociation may become important. It will be of interest to study dissociation arising from gluon radiation of higher multipolarity in future work.

If we place a  $J/\psi$  in a quark-gluon plasma at a temperature  $T$ , the average E1 dissociation cross section is

$$h_{\text{dis}}^{\text{E1}} = \frac{g_g}{2^2} \int_0^{Z-1} h_{\text{dis}}^{\text{E1}}(p) \frac{p^2 dp}{e^{p=T}} n_g; \quad (29)$$

where  $g_g = 16$  is the gluon degeneracy and  $n_g$  is the gluon density,

$$n_g = \frac{g_g}{2^2} \int_0^{Z-1} \frac{p^2 dp}{e^{p=T}}; \quad (30)$$

Using the energy dependence of the dissociation cross section as given in Fig. 10, we can calculate the average dissociation cross section  $h_{\text{dis}}^{\text{E1}}$ . From  $h_{\text{dis}}^{\text{E1}}$ , we obtain the rate of  $J/\psi$  dissociation (by E1 transition) given by

$$\frac{dn_{J/\psi}}{dt} = n_g h_{\text{dis}}^{\text{E1}}; \quad (31)$$

This dissociation rate leads to the collisional dissociation width  $\sigma_{\text{E1}}$  due to the absorption of E1 gluon radiation,

$$\sigma_{\text{E1}} = n_g h_{\text{dis}}^{\text{E1}}; \quad (32)$$

We show in Fig. 11 the temperature dependence of  $h_{\text{dis}}^{\text{E1}}$  and  $\sigma_{\text{E1}}$ . One observes that the average cross section is in the range of 0.5-2 mb. The collisional dissociation width due to E1 gluon absorption is of the order of 0.4 GeV, and the mean life of  $J/\psi$  in the quark-gluon plasma due to the absorption of gluons to the 1P state is therefore of order 0.5 fm/c.

One can assess the stability of  $J/\psi$  in the presence of such a large collisional dissociation width. The quarkonium will be stable if its binding energy is much greater than its dissociation width. It is highly unstable if its dissociation width is much greater than its binding energy. The comparison of the binding energy with the collisional dissociation width provides an assessment of the stability of the quarkonium. We plot in Fig. 11 (b) the binding energy of  $J/\psi$  as a function of temperature. The binding energy is equal to the collisional dissociation width  $\sigma_{\text{E1}}$  at  $T = 1.2 T_c$ ,

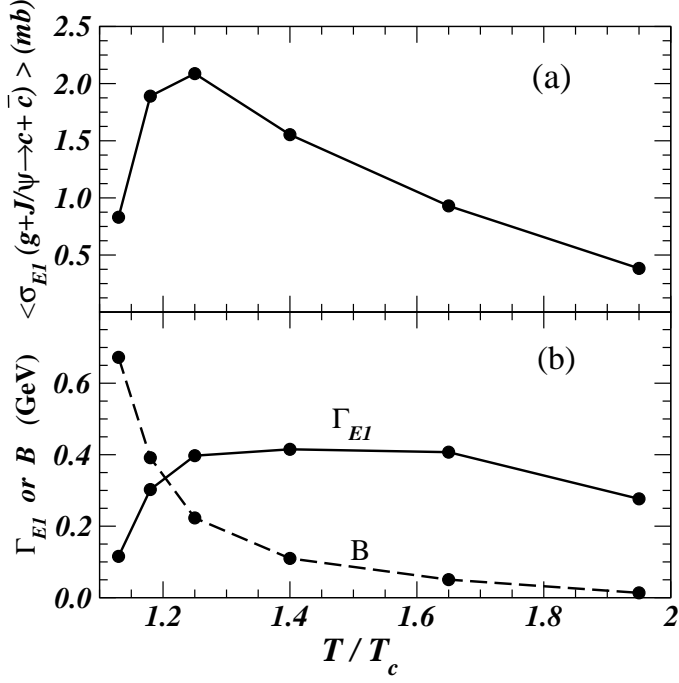


FIG. 11: (a) Thermally averaged dissociation cross section as a function of temperature. (b)  $J/E_1$  collisional dissociation width and  $J/E_1$  binding energy  $B$  as a function of temperature.

and the width becomes much greater than its binding energy as the temperature increases. We infer that the  $J/E_1$  quarkonium will be unstable against dissociation by collision with gluons when the temperature of the quark-gluon plasma greatly exceeds  $1.2T_c$ .

One can make an additional assessment on the stability of a heavy quarkonium by comparing its binding energies with the temperature, as the heavy quarkonium can dissociate by thermalization in the quark-gluon plasma [18, 19, 20]. Dissociation by thermalization refers to the excitation of the bound system into unbound resonance states of the quarkonium system in which the  $Q$  and the antiquark  $\bar{Q}$  remains in the vicinity of each other while the dissociation by collision refers to the excitation into unbound continuum states of  $Q$  and  $\bar{Q}$ . The heavy quarkonium is highly unstable if the binding energy is much smaller than the temperature. From Fig. 11, we note that the binding energy of  $J/E_1$  is equal to the temperature of the quark-gluon plasma at  $T = 1.2T_c$  and the binding energy becomes less than the temperature at higher temperatures. We infer again that the heavy quarkonium is unstable against thermalization at temperatures much higher than  $1.2T_c$ .

#### X. $J/E_1$ PRODUCTION BY C-C IN QGP

In high-energy nuclear collisions, elementary nucleon-nucleon collisions lead to the production of open heavy quark mesons. Although the probability for such a production is small for a single nucleon-nucleon collision, there are many nucleon-nucleon collisions in a central nucleus-nucleus collision. The large number of binary nucleon-nucleon collisions can produce many pairs of open charm mesons, and these open charm mesons can recombine to produce  $J/E_1$ . It is of interest to estimate the elementary reaction cross section for  $c + c \rightarrow J/E_1 + g$  and obtain the rate of  $J/E_1$  production in a nucleus-nucleus collision.

The reaction  $c + c \rightarrow J/E_1 + g$  is just the inverse of  $g + J/E_1 \rightarrow c + c$ . Their cross sections are therefore related by [73]

$$^{E_1}(c + c \rightarrow J/E_1 + g) = \frac{\vec{p}_1 \cdot \vec{p}_2}{\vec{p}_3 \cdot \vec{p}_4} ^{E_1}(J/E_1 + g \rightarrow c + c); \quad (33)$$

where  $\vec{p}_1$  is the momentum of one of the particles in the  $J/E_1 + g$  system, and  $\vec{p}_3$  is the momentum of one of the particles in the  $c + c$  system, both measured in the center-of-mass frame. With Eq. (33) and the results of  $^{E_1}(J/E_1 + g \rightarrow c + c)$  in Fig. 10, the production cross section  $^{E_1}(c + c \rightarrow J/E_1 + g)$  can be calculated. The cross section as a function of

the kinetic energy of  $c$  and  $\bar{c}$  in the center-of-mass system are shown in Fig. 12. One observes that the cross section peaks at low kinetic energies near the threshold, and the magnitude of the cross section decreases with temperature. The maximum cross section at  $T=T_c$  1:13 is of order 4 mb.

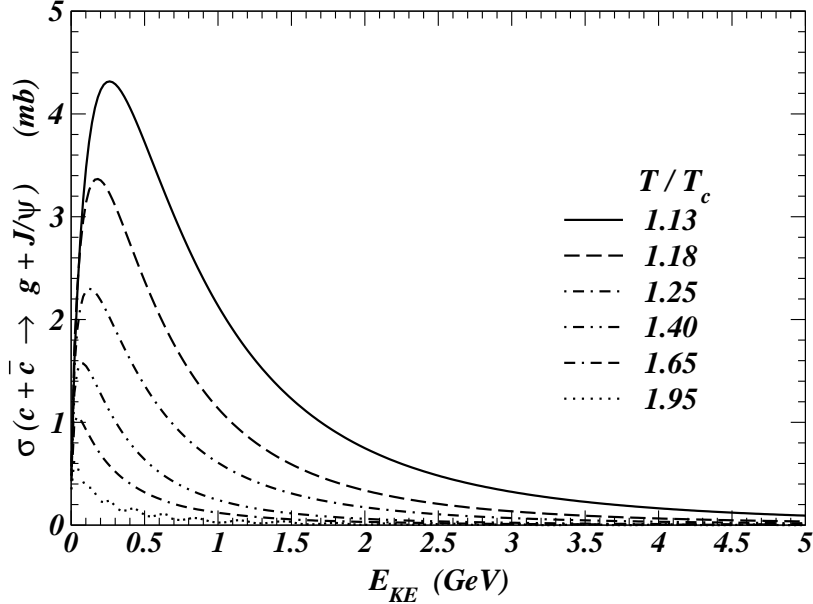


FIG. 12: Cross section for the production of  $J/\psi$  by the collision of  $c$  and  $\bar{c}$

The rate of  $J/\psi$  production can be obtained when the momentum distribution  $f(y; p_t)$  of the produced  $c$  and  $\bar{c}$  is known. For simplicity, we consider charm quarks and antiquarks to be contained in a spatial volume  $V$  with a uniform distribution. The probability of producing a  $J/\psi$  in the volume  $V$  per unit time by the collision of charm quark and antiquark is  $(c + \bar{c})! J/\psi + g) v_{12} = V$ , where  $v_{12}$  is the relative velocity between  $c$  and  $\bar{c}$ . The number of  $J/\psi$  produced per unit time from collision of  $c$  and  $\bar{c}$  is therefore

$$\frac{dN_{J/\psi}}{dt} = \int dy_1 dp_{1t} dy_2 dp_{2t} f(y_1; p_{1t}) f(y_2; p_{2t}) (c + \bar{c})! J/\psi + g) v_{12} = V : \quad (34)$$

When we neglect initial- and final-state interactions, the momentum distribution of charm is given by

$$f(y; p_t) = N_{\text{bin}} \frac{E dN_{cc}^{\text{pp}}}{dp} \quad (35)$$

Here  $f(y; p_t)$  is normalized to the total number of charm quarks  $N_c$  and antiquarks  $N_{\bar{c}}$  produced in the nucleus-nucleus collision,  $N_c = N_{\bar{c}} = (dp=E) f(y; p_t) = N_{\text{bin}} N_{cc}^{\text{pp}}$ ,  $N_{\text{bin}}$  is the number of binary nucleon-nucleon collisions, and  $N_{cc}^{\text{pp}}$  is the number of  $cc$  pair produced in a single nucleon-nucleon collision. From the charm production data in  $d\text{-A}/d\text{p}_t$  and PYTHIA calculations, Tai et al: [74], Adams et al: [75], and the STAR Collaboration inferred that at  $\sqrt{s} = 200$  GeV the charm production cross section per nucleon-nucleon collision is  $\frac{dN_{cc}^{\text{pp}}}{dp} \text{STAR} = 1.18 \pm 0.21 \text{ (stat)} \pm 0.39 \text{ (sys)} \text{ mb}$  [74] and  $\frac{dN_{cc}^{\text{pp}}}{dp} \text{STAR} = 1.4 \pm 0.2 \pm 0.4 \text{ mb}$  [75]. If one uses the transverse momentum distribution measured and parameterized by Tai et al: [74] and assumes a Gaussian rapidity distribution, the charm momentum distribution of Adams et al: [75] per nucleon-nucleon collision can be represented by

$$\frac{E dN_{cc}^{\text{pp}}}{dp} \text{STAR} = \frac{E dN_{cc}^{\text{pp}} \text{STAR}}{dp \text{ in}} = A \frac{e^{-y^2/2}}{(1 + p_t/p_{t0})^n}; \quad (36)$$

where  $\text{in} = 42 \text{ mb}$  is the nucleon-nucleon inelastic cross section,  $A = 4.4 \cdot 10^{-3} (\text{GeV}^{-2})$ ,  $y = 1.84$ ,  $p_{t0} = 3.5 \text{ GeV}$ , and  $n = 8.3$ . The number of  $cc$  produced per nucleon-nucleon collision is  $N_{cc}^{\text{pp}} \text{STAR} = 1.4 \text{ mb}/42 \text{ mb} = 0.033 \pm 0.0107$ .

The PHENIX Collaboration obtained  $\frac{dN_{cc}^{\text{pp}}}{dp} \text{PHENIX} = 622 \pm 57 \text{ (stat)} \pm 160 \text{ (sys)} \text{ mb}$  [76] for the open charm production cross section per nucleon-nucleon collision at  $\sqrt{s} = 200 \text{ GeV}$ , and  $N_{cc}^{\text{pp}} \text{PHENIX} = 0.0148 \pm 0.004$ . With this total charm production cross section, the theoretical results from the PYTHIA calculations can be parameterized as [76, 77]

$$\frac{E dN_{cc}^{\text{pp}}}{dp} \text{PHENIX} = \frac{a_0 (1 + a_3 p_t)}{\exp[a_1 p_t^2 + a_2 p_t g_2]} (e^{a_4 y^2} + a_5 + a_6 e^{a_7 y^2}); \quad (37)$$

where  $a_0 = 4.05 \cdot 10^{-5}$  (GeV<sup>-1</sup>),  $a_1 = 0.157$  (GeV<sup>-2</sup>),  $a_2 = 0.54$  (GeV<sup>-1</sup>),  $a_3 = 11967.3$  (GeV<sup>-1</sup>),  $a_4 = 0.003633$ ,  $a_5 = 0.00965$ ,  $a_6 = 1.003914$ , and  $a_7 = 0.003554$ . We shall focus attention to a central collision consisting of the most inelastic 10% of the reaction cross section. The average number of binary collision  $N_{\text{bin}}$  for such a central collision is  $N_{\text{bin}} = 833$ . For this central nucleus-nucleus collision at  $\sqrt{s} = 200$  GeV, the number of c and c produced is  $N_c = N_{\bar{c}} = 27.8 \pm 8.9$  if we use the cross section of the STAR Collaboration [75], and  $N_c = N_{\bar{c}} = 12.34 \pm 3.4$  if we use the cross section of the PHENIX Collaboration [76]. The rate of  $J/\psi$  production can then be obtained from Eqs. (34)–(37) by carrying out the six-fold integration. We show the quantity  $V dN_{J/\psi} / dt$  as a function of temperature for the most inelastic (10%) central Au-Au collision at  $\sqrt{s} = 200$  GeV in Fig. 13.

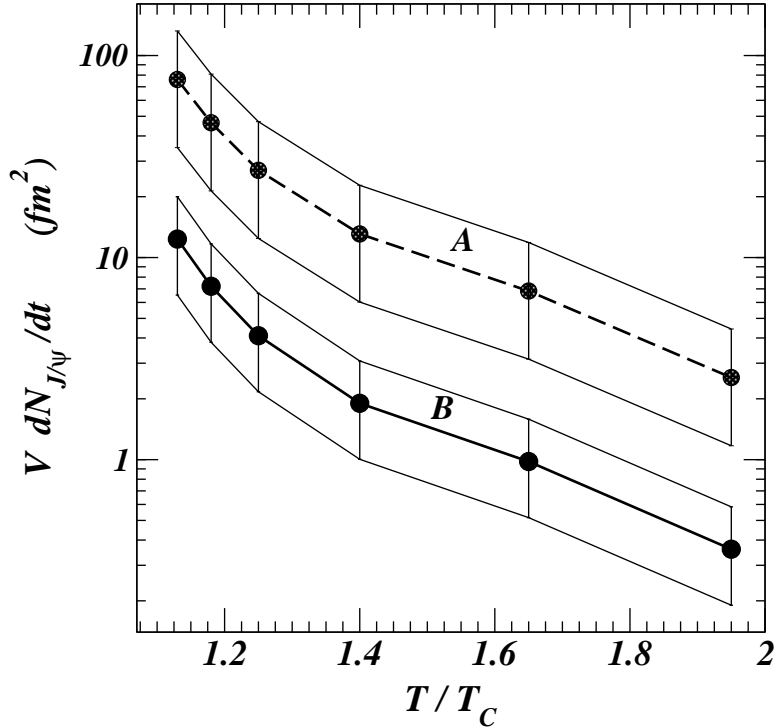


FIG. 13: The rate of  $J/\psi$  production as a function of temperature, for the most inelastic (10%) central Au-Au collision at  $\sqrt{s} = 200$  GeV. Curve A is based on the parametrization of Eq. (36) using the total charm cross section of the STAR Collaboration [75] and Curve B is based on the PYTHIA parametrization of Eq. (37) using the total charm cross section of the PHENIX Collaboration [75, 77].

We can illustrate the magnitude of  $J/\psi$  by considering a Au-Au central collision with a transverse area of  $(7 \text{ fm})^2$  and a longitudinal initial time (and longitudinal length) of 1 fm. The initial volume containing the charm quarks and antiquarks is about  $150 \text{ fm}^3$ . If the initial temperature is 0.4 GeV, the initial rate of  $J/\psi$  production will be about 1/15 to 1/100 (fm/c)<sup>2</sup>. As the volume expands, the temperature decreases. The results of Fig. 13 can be used to provide an estimate of the rate of  $J/\psi$  production.

## X I. DISCUSSIONS AND CONCLUSIONS

We use the color-singlet Q-Q potential obtained by Kaczmarek et al. [17] in quenched QCD to study the energy levels of charmonium and bottomium above the phase transition temperature. The potential extracted from the lattice-gauge calculations indicates a very strong coupling between the heavy quark and the gluon at temperatures slightly greater than the phase transition temperature. Such a strong coupling leads to an attractive potential and the strong binding of these quarkonia. We find that  $J/\psi$ ,  $c\bar{c}$ ,  $b\bar{b}$ , and  $\Lambda_b\bar{\Lambda}_b$  are bound at temperatures just above  $T_c$ . For example, at  $T = T_c = 1.13$ , the binding energy of  $J/\psi$  and  $c\bar{c}$  are 0.7 and 2.8 GeV respectively, and the binding energies of  $(c\bar{c})$  and  $(b\bar{b})$  are 0.05 GeV and 0.5 GeV respectively.

The strong coupling of Q and Q at  $T$  slightly above  $T_c$  led us to study the antiscreening effects due to deconfined gluons. We found that because the Gauss law of QCD contains a non-linear term involving the gluon field, color charges

are induced at the end points. These induced color charges act to antiscreen the interaction between the heavy quark and the antiquark. The strength of the antiscreening effects increases with an increase in the gluon correlation length and is proportional quadratically to the magnitude of the gluon field. Because of the large correlation length at the onset of the phase transition and the sudden increase in the density of deconfined gluons, the antiscreening effects due to deconfined gluons may be the origin of the strong coupling of the quark and antiquark at  $T$  slightly above  $T_c$ .

The quarkonium  $^0$  and  $^0$  becomes unbound at  $1.2 T_c$ ,  $J=$  at  $2 T_c$ ,  $^0$  and  $^0$  at  $2 T_c$ , and at  $4.5 T_c$ . Within the same quenched approximation, these results support the qualitative features concerning the stability of heavy quarkonia in the spectral analyses of Sakawa et al: [6, 7] and Petreczky et al: [8, 9, 10], although there are quantitative differences in the locations of the dissociation temperatures.

It is not necessary to reach the temperature for spontaneous dissociation with zero binding energy for a quarkonium to dissociate. The quarkonium can dissociate at lower temperatures by collision with gluons in the quark-gluon plasma. We are well advised to study the dissociation of quarkonium in collision with gluons. Using the wave functions obtained in the bound state analysis and adopting a simple generalization of the color-octet potential from the color-singlet potential, we calculate the  $J=$  dissociation cross section by assuming that the gluon-(heavy quark) coupling for the dissociation process has the same strength as the coupling for the binding of the quarkonium. The thermally average  $J=$  dissociation cross section then turns out to range from 0.5 mb to about 2 mb for temperatures from 1.1 to  $2 T_c$ .

On the other hand, the density of the gluons is quite large, because of the high level of degeneracies of the gluons. The large gluon density in conjunction with the dissociation cross section of order 1 mb leads to a collisional dissociation width of order 0.4 GeV. The comparison of the collisional dissociation width with the magnitude of the binding energy reveals indeed that collisional dissociation is an important instability even at temperatures below the onset of spontaneous dissociation.  $J=$  is unstable against dissociation by collision with gluons when the temperature of the quark-gluon plasma is much greater than  $1.2 T_c$ . An additional assessment on the instability of  $J=$  can be made by comparing its binding energy with the temperature. Such a comparison also indicates that  $J=$  is unstable against dissociation by thermalization when its temperature far exceeds  $1.2 T_c$ .

In a nucleus-nucleus collision, charm quarks and antiquarks are produced in the hard-scattering process in nucleon-nucleon collisions. During the time of a central nuclear reaction, the charm quark and antiquark will be present in the quark-gluon plasma. They can interact and form  $J=$ . We have calculated the cross section for  $J=$  production by the collision of charm quark and antiquark. The cross section is energy dependent, and the maximum cross section increases as the temperature decreases. The production cross section can be used to study the rate of  $J=$  production in nucleus-nucleus collisions.

We have carried out the investigation using the quenched QCD. It will be of interest to carry out similar investigations using unquenched QCD. Results of the full QCD in two flavors [67] and in three flavors [78] have been obtained recently, and an investigation on  $J=$  dissociation temperatures in QCD with two flavors has been initiated [12]. A thorough study of how the dynamical quarks will affect the stability, the dissociation, and the inverse production of heavy quarkonium will be of great interest.

#### Acknowledgments

The authors would like to thank Drs. P. Petreczky, M. Gyulassy, Sung Hoon Lee, T. Barnes, S. Ohta, V. Cianciolo, D. Silvermyr, Huan Huang, and Zhangbu Xu for helpful discussions and communications. This research was supported in part by the Division of Nuclear Physics, U.S. Department of Energy, under Contract No. DE-AC05-000R22725, managed by UT-Battelle, LLC.

---

- [1] T. Matsui and H. Satz, Phys. Lett. B 178, 416 (1986).
- [2] C. D. Etar, Phys. Rev. D 32, 276 (1985).
- [3] C. D. Etar, Phys. Rev. D 37, 2328 (1988).
- [4] T. H. Hansson, S. H. Lee, and I. Zahed Phys. Rev. D , 37, 2672 (1988).
- [5] F. Karsch and E. Laermann, Chapter to appear in Quark-Gluon Plasma III, R. Hwa (ed.), hep-lat/0305025.
- [6] M. A. Sakawa, T. H. Matsuda, and Y. Nakahara Nucl. Phys. A 715, 863 (2003).
- [7] M. A. Sakawa and T. H. Matsuda, Phys. Rev. Lett. 92, 012001 (2004).
- [8] P. Petreczky, S. Datta, F. Karsch, and I. Wetzorke, hep-lat/0309012.
- [9] S. Datta, F. Karsch, P. Petreczky, and I. Wetzorke, hep-lat/0312037.
- [10] P. Petreczky, J. Phys. G 30 S431-S440 (2004), hep-ph/0305189.
- [11] E. V. Shuryak and I. Zahed, hep-ph/0307267.
- [12] E. V. Shuryak and I. Zahed, hep-ph/0403127.

[13] E.V. Shuryak, [hep-ph/0405066](#).

[14] E.V. Shuryak and I. Zahed, [hep-ph/0406100](#).

[15] T. Hatsuda and T. Kunihiro, *Phys. Rev. Lett.* **55**, (1985) 158; T. Hatsuda and T. Kunihiro, *Prog. Theor. Phys.* **74**, (1985) 765.

[16] L.G randchamp, R.Rapp, G.E.Brown, *J. Phys. G*, **30** S1355 (2004);

[17] O.Kaczmarek, F.Karsch, P.Petreczky, and F.Zantow [hep-lat/0309121](#).

[18] D.Kharzeev, L.McLerran, and H.Satz, *Phys. Lett. B* **356**, 349 (1995).

[19] C.Y.Wong, *Phys. Rev. C* **65**, 034902 (2002).

[20] C.Y.Wong, *J. Phys. G* **28**, 2349 (2002).

[21] R.L.Thews, M.Schroedter, and J.Rafelski, *Phys. Rev. C* **63**, 054905 (2001).

[22] R.L.Thews and J.Rafelski, *Nucl. Phys. A* **698**, 575 (2002).

[23] S.Digal, D.Petreczky, and H.Satz, *Phys. Lett. B* **514**, 57 (2001) [[hep-ph/0105234](#)].

[24] S.Digal, D.Petreczky, and H.Satz, *Phys. Rev. D* **64**, 094015 (2001) [[hep-ph/0106017](#)].

[25] F.Zantow, O.Kaczmarek, F.Karsch, and P.Petreczky, [hep-lat/0301015](#).

[26] K.H.Ackermann et al., STAR Collaboration, *Phys. Rev. Lett.* **86**, 402 (2001); C.Adler et al., STAR Collaboration, *Phys. Rev. Lett.* **87**, 182301 (2001); R.Snellings for the STAR Collaboration, *Nucl. Phys. A* **698**, 193c (2002).

[27] R.A.Lacey for the PHENIX Collaboration, *Nucl. Phys. A* **698**, 559c (2002); K.Adox et al., PHENIX Collaboration, [nucl-ex/0204005](#).

[28] I.C.Park for the PHOBOS Collaboration, *Nucl. Phys. A* **698**, 564c (2002).

[29] P.F.Kolb, J.Sollfrank, and U.Heinz, *Phys. Lett. B* **459**, 667 (1999) and *Phys. Rev. C* **62**, 054909 (2000); P.F.Kolb, P.Huovinen, U.Heinz, and H.Heiselberg, *Phys. Lett. B* **500**, 232 (2001); P.F.Kolb, U.Heinz, P.Huovinen, K.J.Eskola, and K.Tuominen, *Nucl. Phys. A* **696**, 197 (2001); P.Huovinen, P.F.Kolb, U.Heinz, P.V.Ruuskanen, and S.A.Voloshin, *Phys. Lett. B* **503**, 58 (2001); P.Kolb and U.Heinz, [nucl-th/0305084](#).

[30] T.Hirano, *Phys. Rev. C* **65**, 011901 (2001); T.Hirano, *Phys. Rev. C* **65**, 011901 (2001); T.Hirano, K.Tsuda, *Phys. Rev. C* **66**, 054905 (2002); T.Hirano, [nucl-th/0410017](#).

[31] D.Teaney, J.Lauret, and E.V.Shuryak, *Phys. Rev. Lett.* **86** 4783 (2001); D.Teaney, J.Lauret, and E.V.Shuryak, [nucl-th/0110037](#); D.Teaney, *Phys. Rev. C* **68**, 034913 (2003).

[32] L.D.Landau, *Izv. Akad. Nauk SSSR* **17**, 52 (1953); L.D.Landau and S.Z.Belenkij, *Usp. Fiz. Nauk.* **56**, 309 (1955).

[33] P.Carnuthers, M.Duong-Van, *Phys. Rev. D* **8**, 859 (1973).

[34] M.Murray, the BRAHMS Collaboration, *J. Phys. G* **30**, S667-S674 (2004).

[35] S.M.H.Wong, [hep-ph/0404222](#).

[36] D.Molnar and M.Gyulassy, [nucl-th/0102031](#); D.Molnar and M.Gyulassy, *Nucl. Phys. A* **698**, 379 (2002); D.Molnar and M.Gyulassy, *Nucl. Phys. A* **697**, 495 (2002).

[37] E.Shuryak, *Prog. Part. Nucl. Phys.* **53**, 273 (2004).

[38] M.Gyulassy and L.McLerran, [nucl-th/0405013](#), to be published in *Nucl. Phys. A*.

[39] New Discoveries at RHIC: the current case for the strongly interactive QGP, RIKEN Scientific Articles, Volume 9, BNL, May 14-15, 2004.

[40] Ziwei Lin, C.M.Ko, and S.Pal, *Phys. Rev. Lett.* **89**, 152301 (2002).

[41] G.T.Bodwin, E.Braaten, and G.P.Lepage, *Phys. Rev. D* **51**, 1125 (1995).

[42] C.Y.Wong, *Phys. Rev. D* **60**, 114025 (1999).

[43] T.Appelquist, M.Dine, and I.Muzinich, *Phys. Lett. 69 B*, 231 (1977).

[44] S.Love, *Ann. Phys. (N.Y.)* **113**, 153 (1978).

[45] R.Barbieri, M.Ciafaloni, and P.Menotti, *Nuovo Cim.* **55A**, 701 (1968).

[46] V.B.Berezetskii, E.M.Lifshitz, and L.Pitaevskii, *Quantum Electrodynamics*, Pergamon Press, 1982.

[47] Yongseok Oh, Sungsik Kim, Sung Young Lee, *Phys. Rev. C* **65**, 067901 (2002).

[48] V.V.Klimov, *Yad. Fiz.* **33**, 1734 (1981) [*Sov. J. Nucl. Phys.* **33**, 934 (1981)]

[49] H.A.Weldon, *Phys. Rev. D* **26**, 2789 (1982).

[50] J.I.Kapusta, *Finite Temperature Field Theory*, Cambridge Press, 1989.

[51] E.Braaten and R.D.Pisarski, *Phys. Rev. D* **45**, 1827 (1992).

[52] A.Rebhan, *Phys. Rev. D* **48**, 3967 (1993).

[53] F.Karsch, Lectures given at 40th Internationale Universitatswochen fuer Theoretische Physik: Dense Matter (IUKT 40), Schladming, Styria, Austria, 3-10 Mar 2001, [hep-lat/0106019](#).

[54] K.Gottfried and V.F.Wesskopf, *Concepts of Particle Physics*, Oxford University Press, New York, 1986, Vol. II, page 385.

[55] M.Peskin and D.V.Schroeder, *An Introduction to Quantum Field Theory*, Addison-Wesley, Reading, Massachusetts, 1996, page 542.

[56] B.Svetitsky and L.Yaffe, *Nucl. Phys. B* **210**, 423 (1982).

[57] L.G.Yaffe and B.Svetitsky, *Phys. Rev. D* **26**, 963 (1982).

[58] T.A.Degrand and C.E.DelTar, *Phys. Rev. D* **8**, 2469 (1986).

[59] J.B.Kogut et al., *Phys. Rev. Lett.* **50**, 393 (1983).

[60] C.E.DelTar and J.B.Kogut, *Phys. Rev. Lett.* **59**, 399 (1987); *Phys. Rev. D* **36**, 2828 (1987); S.Gottlieb et al., *Phys. Rev. Lett.* **59**, 1881 (1987).

[61] M.Fukugita et al., *Phys. Rev. Lett.* **63**, 1768 (1989).

[62] K.Holland, M.Pepe, and U.-J.Wiese, *Nucl. Phys. B* **694**, 35 (2004).

- [63] F. Karsch, E. Laermann, and M. Lutgemeier, Phys. Lett. B 346, 94 (1995).
- [64] Sung H. Lee, Phys. rev. D 40, 2484 (1989).
- [65] J. M. Yedomans, *Statistical Mechanics of Phase Transitions*, Clarendon Press, Oxford, 1992.
- [66] K. Hagiwara et al., the Particle Data Group, Phys. Rev. D 66, 010001 (2002).
- [67] O. Kaczmarek, S. E. Jiri, F. Karsch, E. Laermann, and F. Zantow hep-lat/0312015.
- [68] C. Y. Wong, E. S. Swanson, and T. Barnes, Phys. Rev. C 65, 014903 (2001).
- [69] M. E. Peskin, Nucl. Phys. B 156, 365 (1979).
- [70] G. Bhanot and M. E. Peskin, Nucl. Phys. B 156, 391 (1979).
- [71] J. M. Bhatt and V. F. Weisskopf, *Theoretical Nuclear Physics*, John Wiley & Sons, New York, 1952, Eq. (V III 2.63), page 334.
- [72] D. Kharzeev and H. Satz, Phys. Lett. B 334, 155 (1994).
- [73] Page 337 of Ref. [71].
- [74] A. Tai, the STAR Collaboration, J. Phys. G 30, S809 (2004).
- [75] J. Adams, et al., the STAR Collaboration, nucl-ex/0407006.
- [76] S. S. Adler, the PHENIX Collaboration, nucl-ex/0409028.
- [77] The author would like to thank Drs. D. Silverman and V. Cianciolo for providing the parametrization of the cc distribution, Eq. (37).
- [78] P. Petreczky and K. Petrow, hep-lat/0405009.